5-2014

A Spatial Analysis of Streambank Heterogeneity and its Contribution to Bank Stability

Paul Vanterpool Simmons
University of Tennessee - Knoxville, psimmon4@utk.edu

To the Graduate Council:

I am submitting herewith a thesis written by Paul Vanterpool Simmons entitled "A Spatial Analysis of Streambank Heterogeneity and its Contribution to Bank Stability." I have examined the final electronic copy of this thesis for form and content and recommend that it be accepted in partial fulfillment of the requirements for the degree of Master of Science, with a major in Environmental Engineering.

John S. Schwartz, Major Professor

We have read this thesis and recommend its acceptance:

Jon Hathaway, Edmund Perfect

Accepted for the Council:
Carolyn R. Hodges

Vice Provost and Dean of the Graduate School

(Original signatures are on file with official student records.)

A Spatial Analysis of Streambank Heterogeneity and its Contribution to Bank Stability

A Thesis Presented for the
Master of Science
Degree
The University of Tennessee, Knoxville

Paul Vanterpool Simmons
May 2014

Abstract

Streambank erosion is a function of fluvial detachment and geotechnical failure mechanisms working in combination to cause bank retreat. It is generally agreed that bank stability is dependent on both types of erosion; however, few studies have attempted to correlate the driving and resisting forces between the two. It has been proposed that: (1) streambanks possess a spatial structure and dependence of non-erodible resistant structures such as root masses and rocks; (2) streambanks naturally “armor” themselves from fluvial erosion with a combination of hard points and resistive soil; and (3) the stability of the streambank can be predicted by the amount of composite fluvial resistance, thereby connecting fluvial resistance and geotechnical stability. These hypotheses were tested through extensive field analysis, spatial statistical methods, and multivariate statistics. Eighteen streambanks sites with cohesive sediment structures in the Eastern Tennessee Ridge and Valley Ecoregion were sampled for in-situ erodibility and critical shear stress as well as the spatial distribution of non-erodible hard points. Using a combination of nearest neighbor, join count, and indicator variogram statistics it was discovered that streambanks in this region possess natural clusters of these non-erodible structures. However, the study was unsuccessful in determining the cause of spatial dependency of non-erodible clusters between various banks, as not all banks exhibit this quality. Multiple linear regression was utilized to compare all streambanks, with the results indicating that the density of these clustered hard points displays a positive linear relationship with the critical shear strength of the surrounding soil matrix, suggesting a coordination between the two and possible natural armoring of the composite bank structure. Additionally, the USDA Bank Stability and Toe Erosion Model (BSTEM) was utilized to determine the relative stability of these streambanks. With this information, both discriminate analysis and multiple linear regression were applied to determine that stable streambanks are controlled by a combination of the respective stream power, average soil critical shear strength, standard deviation of the

critical shear strength, bank height, and cluster density of non-erodible structures. This information helped derive relevant interactions for stable stream bank analysis including possible stream restoration and site investigation applications.

Table of Contents

List of Tables

List of Figures

Chapter I

Introduction

Since the establishment of the Clean Water Act in 1972, the quality of waterways in the United States has been under increasing scrutiny. Initially, regulations were aimed at eliminating point source pollution; however, regulations have since expanded to encompass nonpoint sources and Total Maximum Daily Loads for pollutants in the waterways (USEPA, 2012). This is in part due to watershed hydromodification caused by urbanization, agricultural practices, and other land use changes which increase pollutants and runoff entering streams, lakes and rivers (Mohamoud et al., 2009). The result of this land use change is often channel erosion, which causes loss of land, habitat (Carline and Klosiewski, 1985; Shields et al., 1994), and additional degradation of water quality through sedimentation (Klein, 1979; Sherer et al., 1992). In the state of Tennessee, sedimentation in second only to *E. coli* as a cause of stream impairment, accounting for approximately 46% of all impaired stream miles (USEPA, 2010). Excessive sediment loadings can be detrimental to streams and rivers due to physical, chemical, and biological impairment, costing up to $16 billion annually in North America (Osterkamp et al., 1998). This sediment transported within the waterway is delivered from a variety of sources such as upland disturbances, hill slope erosion, and bed degradation (Julien, 2010); however, streambank erosion has been found to be one of the most significant sources, contributing up to 80% of the total sediment load in some systems (Simon and Rinaldi, 2006). For these reasons, streambank protection is a commonly stated objective in stream restoration initiatives (Brown, 2000; Niezgoda et al., 2005; Rosgen, 2007; Shields et al. 2003; Simon et al., 2011). Therefore, there is a need to improve stream restoration design criteria and more comprehensively understand the natural parameters which control bank stability.

Streambank erosion is a complex phenomenon which can be conceptually understood in terms of driving and resisting forces (Simon et al., 2000). From an elementary standpoint, when the force acting upon the bank is greater than the resistant force, erosion will occur (ASCE, 1998a; Simon et al., 2000; Thorne, 1982). The parameters which control these relationships are numerous, varying both spatially and temporally, and are highly dependent on site specific conditions (ASCE, 1998a; Parker et al., 2008). A combination of these variables governs the three main processes contributing to streambank retreat: fluvial erosion, mass failure, and subaerial processes (Lawler, 1995; Thorne, 1982).

The processes of mass failure, fluvial entrainment, and subaerial processes are not independent of one another, all working in combination to destabilize a streambank (Lawler, 1995; Simon et al., 2000). The link between mass failure and fluvial erosion is conceptually recognized as the circular processes of scour of the toe causing massive failure and subsequent toe reinforcement before repeating until the channel reaches a quasi-equilibrium (Thorne, 1982). The extent of this relationship, in regards to the parameters dictating each of the two bank mechanisms, is inadequately understood. Therefore the degree to which composite fluvial resistance controls geotechnical stability is desired. Geotechnical resistance is primarily a function of the bank geometry, soil properties, groundwater, vegetative and water surface conditions (Simon et al., 2000). Fluvial resistance is derived from the strength of the soil matrix (Clark and Wynn, 2006; Simon et al., 2000), flow velocity reductions caused by vegetation (Järvelä, 2002) and non-erodible structures along a streambank such as root masses rock structures. These resistant, non-erodible, points are unaffected by fluvial entrainment and their presence suggests possible geotechnical reinforcement through embedded roots and rocks. In combination with the soil structures, the architecture of these resistance points is believed to affect the degree of bank stability both fluvially and geotechnically. The interaction

between these parameters has not yet been characterized in research, and is therefore the topic of this study.

The focus of this study is to capture an accurate measure of stream bank heterogeneity through rigorous sampling efforts and develop a correlation between this heterogeneity and the integrity of the bank structure through data analysis. This is an exploratory investigation into a complex natural phenomena in which the primary emphasis is to characterize the spatial distribution of non-erodible 'hard' points and relate this information to the streambank properties and stability of the bank. The main hypothesis of this investigation is that streambank stability can be predicted through a combination of contributing parameters and the spatial distribution of non-erodible 'hard points'. The underlying question asked by this study is to what extent does the heterogeneity of stream bank structure and the presence of resistant points contribute to bank stability? This research extends the scientific knowledge of streambank stability and its associated parameters developed by previous research initiatives. To the knowledge of the researcher, a spatial analysis of streambank non-erodible structures has not been completed before and the integration of this knowledge with bank stability principles is a crucial step in fully understanding the interaction of fluvial erosion and massive bank failure.

Chapter II

Background

The following sections have been provided in an effort to present a conceptual understanding of streambank stability and its geological, ecological, and hydrological parameters so that a foundation for a relevant study design can be constructed.

2.1 Streambank Failure Mechanisms

The stability of a natural streambank is highly complex and influenced by a variety of spatial and temporal parameters such as soil characteristics, channel geometry, flow conditions, riparian vegetation, channel state, hydrologic events, water table location, and direct changes to local environment (ASCE 1998a, Eaton and Giles 2009, Fox et al. 2007, Osman and Thorne 1988, Simon and Collison 2002, Thorne 1982, Thorne and Osman 1988, Ullrich 1986). A combination of these variables governs the three main processes contributing to streambank retreat: fluvial erosion, mass failure, and subaerial processes (Abernethy and Rutherford, 1998; Lawler, 1995; Thorne 1982).

Fluvial erosion transpires when the flow in a channel exerts a shear force on the bank face or toe greater than the soil's resistant strength, such that particles and aggregates detach (ASCE 1998a). The average boundary shear force acting upon the soil is a function of channel geometry and flow conditions which can be simplified by the following relationship (Julien, 2010; Simon et al., 2011):

$$\tau = \gamma_w RS \quad (1)$$

where τ = average boundary shear stress (Pa); γ_w = unit weight of water (9.81 kN m^{-3}); R = local hydraulic radius (m); S = channel slope (m m^{-1}). The subsequent erosion resulting from an excess driving force is often described to occur at a rate defined by the excess stress equation:

$$E_r = k_d(\tau - \tau_c)^a \quad (2)$$

where E_r = lateral erosion rate (m/s); k_d = erodibility coefficient (m^3/N-s); τ = applied shear stress (Pa); τ_c = critical shear stress (Pa); and a is an experimental exponent usually assumed to be in unity (Hanson and Cook, 2004; Hanson and Simon, 2001).

The massive failure of a streambank is typically a geotechnical failure in which the driving force of gravity acts on the bank mass, exceeding the resisting soil strength. This driving force can be denoted by a simplified relationship of the bank geometry and soil parameters:

$$s_d = W \sin(\beta) \quad (3)$$

where s_d = driving stress (kPa); W = wet weight of soil block per unit area (kN m^{-2}); β = failure plane angle (degrees) (Parker et al, 2008;Simon et al., 2000). Conversely, the resisting shear strength is traditionally represented by the Mohr – Coulomb equation for saturated soil:

$$s_r = c' + (\sigma - \mu_w)tan\phi' \quad (4)$$

where s_r= shear strength of the soil (kPa); c' = effective cohesion (kPa); σ = normal stress (kPa); μ_w = pore-water pressure (kPa); and ϕ' = effective angle of internal friction (degrees). For partially saturated and unsaturated soil, the soil shear strength is increased due to matric suction (negative pore-water pressure) above the water table effectively increasing the apparent cohesion in the soil, Under these circumstances, the modified Mohr-Coulomb equation can be used to more accurately represent the soil strength (Simon and Collison, 2001; Simon et al., 2000):

$$s_r = c' + \sigma \tan\phi' + \psi \tan\phi^b \quad (5)$$

where ψ = matric suction; and ϕ^b is an angular relationship describing the rate of increasing soil strength with increasing matric suction (degrees). This relationship (ϕ^b) is generally between 10 and 20 degrees and approaches ϕ' at saturated conditions.

The final streambank failure mechanism, subaerial processes, is associated with temporal variations in addition to physical and spatial properties. Subaerial processes are a series of weakening and weathering which directly affect the moisture conditions of the soil matrix (ASCE 1998a; Thorne 1982). These processes can be classified by either the reduction of the soil strength through increased soil weight, loss of matric suction and positive pore water pressures due to prolonged exposure to water or by the loosening and detachment of particles and aggregates through the freeze thaw cycle (Simon et al., 2000, Thorne 1982). Therefore, subaerial processes contribute to the mass wasting of a bank along with fluvial erosion due to the weakening of the soil structure and increased erodibility. For this reason, subaerial weathering is often regarded separately and not considered a direct failure mechanism.

Although characteristically different, fluvial entrainment and mass failure are intrinsically linked together and work in coordination to control erosion rates and failure types (ASCE 1998a; Midgley et al,. 2012; Simon et al., 2000; Thorne, 1982). For this reason they are integrated in many geomorphologic channel evolution relationships (Lagendoen, 2008b; Simon, 1989a; Simon and Hupp, 1986a). Conceptually speaking, in an incising river, bed degradation causes an increase in bank height to a point of geotechnical instability, resulting in massive bank failure. The deposited sediment settles at the toe of the bank, effectively reinforcing the bank and increasing stability. Given time and appropriate conditions fluvial entrainment scours the toe, creating an imbalance of bank slope and therefore enough geotechnical instability to cause another mass failure after which the process starts over (Thorne and Osman, 1998a; Thorne,

1982). This circular progression continues until the channel reaches a state of quasi-equilibrium. Despite this general understanding of factors affecting bank stability, the extent to which fluvial resistance and geotechnical stability are linked is insufficiently understood.

2.2 Streambank Sediment Properties

Soil accounts for a majority of the mass within a streambank. Therefore, understanding the sediment structure of the bank is critical to stability analyses. Streambank stability studies are generally classified according to the cohesive nature of the soil mass, due to inherent differences and failure mechanisms between cohesive and non-cohesive sediments (Thorne, 1982). Non-cohesive soils consist of discrete particles bound primarily by frictional resistance. Conversely, cohesive soils possess internal electrochemical bonds which assimilate particles together, thereby creating a stronger soil matrix. Failure in non-cohesive soils is accomplished through the entrainment of discrete particles, while cohesive sediments erode as aggregates (Thorne 1982, Thorne and Osman 1988). This phenomena can be explained through the cohesive nature of the soil binding the particles together, making it unlikely that the driving force will contain enough power to break up the cohesive soil aggregate into individual particles.

The sediment structure within a bank is a result of long term geologic conditions, mineralogical composition, alluvial deposition, stress history, and decomposition processes (El-Ramly et al, 2002). According to Bull (1997), fundamental soil properties which govern interparticle strength are known to vary spatially, influencing the cohesive integrity of the soil and likely making it more erodible. Even in apparently homogenous layers, significant variation is known to occur (El-Ramly et al., 2002; Lacasse and Nadim 1996). Parker et al. (2008) determined that a significant amount of variability exists on both the micro-scale (within a cross section) and the meso-scale (between cross sections) along the same reach. Therefore it can be assumed that most banks possess some degree of inherent diversity. This heterogeneity and

variance of the bank sediment structure can have a significant influence on the stability of the bank, therefore, is important to quantify and further investigate these physical characteristics.

An additional condition frequent in streambanks is the stratification of soil layers due to historical deposition and soil forming processes. Stratified sediment layers vary in size, and can be less than a centimeter in thickness. (Ullrich et al., 1986; Fox et al. 2007). This layering influences pore water movement through the soil structure by creating subsurface channels, or seams, which ultimately can compromise the surrounding sediment structure (Ullrich et al., 1986). Additionally, stratified soil layers may also result in perched water tables, caused by the difference in water retention characteristics, creating a non-uniform distribution of forces and potentially resulting in subsequent failure (Fox et al. 2007). Stratified layers may cause significant bank failure depending on local conditions: however, it is difficult to isolate erosion controlled solely by seepage; therefore, it is often not accounted for when considering bank stabilization (ASCE, 1998a; Fox et al. 2007).

2.3 Effects of Streambank Vegetation

It is universally agreed that river bank vegetation has a significant impact on the stability of a stream bank and the mechanisms which cause retreat and failure; however, prediction of its influence remains a difficult task (Eaton and Giles, 2009; Osman and Thorne, 1988; Pollen, 2007; Simon and Collison, 2002; Thorne and Osman, 1988; Thorne, 1990; Wynn and Mostaghimi, 2006). From a system-wide perspective, it is believed that the authority vegetation has over geomorphologic processes can be attributed to the scale of the stream. Smaller streams are significantly influenced by the presence of vegetation, and as channel size and subsequent volumetric flow rates increase, vegetation’s impact on the system lessens (Abernethy and Rutherford, 1998; Eaton and Giles, 2009).

Vegetation is most commonly regarded as providing increased reinforcement to the bank profile. Roots are weak in compression yet strong in tension. Conversely, soil is strong in compression and weak in tension. Therefore, the presence of roots in the soil matrix increases the overall geotechnical strength of the soil structure (Abernethy and Rutherford, 2001; ASCE, 1998a; Simon and Collison, 2002). Additionally, root mass decreases the soil moisture, resulting in increased cohesion and apparent cohesion due to the development of matric suction (Simon and Collison, 2002; Thorne, 1990). Further research suggests that the optimum vegetative strength conferred to the bank is via a small number of substantial roots opposed to an abundant quantity of lesser roots (Simon and Collison, 2002; Wynn and Mostaghimi, 2006).

In addition to structural reinforcement, vegetation affects the local hydrology of the riparian zone and near bank hydraulic forces. Riparian vegetation alters the local microenvironment through the interception of rainfall and evapotranspiration, effectively protecting soil against rainfall impact and decreasing potential moisture (ASCE, 1998a). The presence of vegetation along a bank increases the bank roughness, decreasing the local velocity and therefore hydraulic shearing stress acting on the surrounding soil structure (Fischenich, 2001; Järvelä, 2002). Vegetative masses are also effectively fluvially non-erodible, with permissible shear stress values approaching that of rock (Fischenich, 2001). In effect, vegetation masses along the bank face act to increase the composite structure against fluvial entrainment while simultaneously providing geotechnical reinforcement.

Although the presence of vegetation is commonly viewed as beneficial to bank stabilization, it does not always act to increase the stability of the bank (Simon and Collison, 2002; Thorne and Osman 1988). For example, the existence of a large tree induces a heavy load on the bank top, increasing the driving force on the bank, potentially causing mass failure (Thorne and Osman, 1988). Additionally, the formation of roots forces soil outward, and if a root comes to occupy a crack or fissure it may expand the cracking feature causing localized failure

(ASCE, 1998a). Like all processes associated with riverbank stabilization, vegetation's influence is localized and site dependent. Furthermore, the effect is bound by the vegetation size, location, type, root size, and seasonal change (Thorne and Osman, 1988).

2.4 Hydraulic and Hydrologic Influences on Streambanks

Bank stability is a derivative of physical components such as soil and vegetation, however it is ultimately controlled by hydrology and stream flow conditions. Streambank failure has often been observed during the recession of the hydrograph due to an imbalance of forces in the bank resulting from increased soil unit weight and the sudden drawdown of the water surface (ASCE, 1998a; Simon et al., 2000). As stated in Section 2.1, the boundary shear stress (Equation 1) is the primary driving force for fluvial entrainment and ultimately the stability of the streambank. This relationship is a function of channel geometry, slope and flow conditions. Evidence of the boundary shear stress significance has been restated throughout this introduction through review of other bank features' association with it. The simplified relationship for boundary shear presented by Equation 1 is adequate for relational purposes and infinitely straight streams; however, it does not account for complex flows and secondary currents created in natural channels by expansion/contractions and sinuosity. Papanicolaou et al. (2007) found that sidewall shear stress acting on a bank possessing secondary currents may be up to two to three times more than a bank without secondary currents. This increase in shear stress is most pertinent near the toe of the bank further signifying its control over bank stability.

Boundary shear stress is important for isolating forces at the local scale; however, channel evolution investigations often develop reach scale relationships to assess stability. One such hydraulic control on stream widening and erosion is the channel forming, or effective, discharge. The channel forming discharge is considered that which governs the size, shape, and sediment transport within a channel and has been correlated with bankfull events in several

studies (Andrews, 1980; Hey, 1982). It is therefore used in stability investigations and for design criteria (Shields et al., 2003). In a study by McPherson (2011), a regional curve to estimate bankfull discharge was developed for the Eastern Tennessee Ridge and Valley Ecoregion, with significance of p=0.0001 and R^2 = 0.96:

$$Q_{bf} = 68.82\ (DA)^{0.77} \quad (6)$$

where Q_{bf} = bankfull flow ($ft^3\ s^{-1}$); and DA = drainage area ($miles^2$)

Regional curves are beneficial for the prediction of bankfull flows and channel geometry in systems where direct measurements are not possible. These relationships are developed for specific regions and are utilized by engineers for stream restoration designs (Rosgen, 1994).

While the hydraulic shear stress acting on the bank is the best indicator of driving force for instability, it is not always easy to define. Therefore, stream power is often used to describe the amount of energy within a stream, subsequent erosion, and sediment transport (Booth, 1990). Stream power represents the energy of flow applied to the stream bed and bank due to the flow of water and the slope. In essence, it is quantifies the ability to accomplish geomorphologic work through sediment detachment and transport (Bagnold, 1966; Goudie, 2013). Therefore, stream power (Ω) has been applied in various models to estimate the amount of deposition and degradation in channels (Neitsch et al., 2005).

$$\Omega = \rho g Q S \quad (7)$$

where ρ = density of water (1,000 kg m^{-3}); g = acceleration due to gravity (9.81 m s^{-2}); Q = volumetric flow rate ($m^3\ s^{-1}$); and S = slope of the stream corridor (m m^{-1}).

Additional modification of Equation (7) has been used by engineers and scientists to further describe the stream power available per unit width. This unit stream power (ω) more

appropriately estimates the average stream power over a unit area (Bagnold, 1966). Therefore, it provides an adequate measure of the erosive capacity for flow in the respective stream (Beschta and Platts, 1986).

$$\omega = \frac{\Omega}{b} = \frac{\rho g Q S}{b} \quad (8)$$

where b = width of the channel (m).

Used in coordination with the bankfull flow, the stream power and unit stream power can be applied assess stability of stream reaches and predict erosion.

Chapter III

Methods

To meet the study objectives, the experimental design involved a multifaceted approach building on the previously introduced principles of natural stream bank structure and stability. This was accomplished by an innovative approach utilizing several techniques including: site selection, BSTEM modeling, bank heterogeneity characterization, in-situ soil shear strength and erodibility determination, Atterberg limits determination, and spatial statistical modeling. The results from these analyses were compared using multivariate statistics to derive pertinent relationships within the data set.

3.1 Site Selection

A total of eighteen streambanks were studied along 1st order to 4th order streams. The selection process of streambank sites for this research was intended to appropriately capture a diverse set of stream bank conditions in the Eastern Tennessee Ridge and Valley Ecoregion. The focus was to select banks, cohesive in nature, which demonstrated non-stratified soil structure to control as many possible mechanisms and variables contributing to bank instability. Therefore, a robust analysis of the heterogeneity of non-erodible structures and soil parameters was accomplished. Seemingly stable and unstable banks were selected from both urban and agricultural regions, and a large variety of bank types (highly vegetated to non-vegetated) was encouraged. The criterion for selection was that the bank exhibit a uniform slope structure and height along straight reaches for a distance of approximately 10 meters. In an effort to minimize temporal changes to the bank geometry, moisture content, and sediment structure, all parameters were measured at a given site within the short time frame of less than 10 days.

3.2 BSTEM Modeling

An integral component of this analysis was determining the relative stability of the streambank. Several different methods were available for this task; however, the USDA Bank Stability and Toe Erosion Model (BSTEM) was selected due to its common usage in stream restoration applications (Simon, 2011) and streambank stability assessments (Pollen, 2007; Simon et al., 2000). This methodology possesses the ability to classify the magnitude of bank stability through Factor of Safety (F_s) determination as well as run time sensitive flow simulations to predict cross sectional changes and erosion rates for composite streambanks. Developed by a collaboration of researchers through a sequence of updates, BSTEM is a Microsoft Excel based spreadsheet tool programed in the Visual Basic language (Pollen-Bankhead and Simon, 2009; Simon et al., 2000; Simon and Collison, 2002; Langendoen and Simon, 2008). It applies a mechanistic bank stability model in an attempt to simulate the complex geotechnical interactions of alluvial streambanks. Input parameters driving the simulation include: bank geometry, soil properties, vegetation, and toe protection (Simon et al., 2011).

Bank geometry input into BSTEM is accomplished through either a detailed land survey of the cross section or by entering the predicted/measured bank angle, bank height, toe angle, and toe height. To satisfy this geometry input requirement and accurately construct an average F_s for each streambank, three cross sectional measurements per bank were taken using a level, rod, and tape surveying equipment. These three cross sections were taken at the upstream and downstream borders as well as the midpoint along the bank reach. This also allowed a verification of the continuity of each streambank, while also providing a more accurate representation of the bank F_s.

The soil parameters used by BSTEM include: critical shear stress (τ_c), effective cohesion (c'), effective friction angle (ϕ'), erodibility (k_d), matric suction (ψ), pore water pressure

(μ_w), and unit weight of sediment (γ_s). These values can be measured directly, however this is costly and not always attainable; therefore, default values are included in the model with selection based on material classification (Simon et al., 2011). A study by Midgley et al. (2012) reviewed the use of BSTEM by comparing measured and predicted results, utilizing both measured and default soil parameters. They discovered that the default fluvial parameters (τ_c and k_d) varied significantly from the measured values, while the default geotechnical parameters were consistent with their measured values. Therefore, it was prudent to apply default values to all geotechnical soil parameters while using in-situ measurements of fluvial soil properties for this study (Section 3.4). The τ_c and k_d values were entered into BSTEM according their mean stratified value based on the location of the measurement Appendix B). This created a more accurate depiction of the bank soil matrix, thereby increasing the accuracy of the results.

Vegetative reinforcement is another input parameter in BSTEM. The amount of additional strength added by roots is estimated through the root reinforcement (RipRoot) sub-model. The RipRoot submodel is a fiber-bundle model developed by Pollen and Simon (2005) and updated by Pollen-Bankhead and Simon (2008). The submodel applies a historical archive of the empirical tensile strengths, sizes, growth patterns, and densities of particular vegetation to a sophisticated model accounting for breakage and pullout forces along with soil structure. Roots tend to assimilate in the upper profile of the bank soil (Abernethy and Rutherfurd, 2001; Wynn et al., 2004), and the RipRoot model accounts for this accordingly by reinforcing the appropriate soil layers. Since BSTEM does not possess a comprehensive dataset for all vegetation in Eastern Tennessee, simplifications of vegetative selection had to be made for each bank site. A review of this selection criterion can be found in Appendix C.

A powerful capability of BSTEM is the ability to quantify a factor of safety (F_s) to enable estimation of the degree of stability. This task is completed by the BSTEM spreadsheet routine

through integration of three limit equilibrium-method models: horizontal layers (Simon and Curini, 1998; Simon et al., 2000), vertical slices (Langendoen and Simon, 2008), and cantilever failures. BSTEM has the capacity to determine a factor of safety for saturated, partially saturated, and unsaturated streambanks by integrating Equations (3), (4), and (5) to develop the following relationship (Simon et al., 2011):

$$F_s = \frac{\sum_{i=1}^{I}\left(c_i' L_i + S_i tan\phi_i^b + [W_i \cos\beta - U_i + P_i cos(\alpha-\beta)]tan\phi_i'\right)}{\sum_{i=1}^{I}(W_i \sin\beta - [\alpha-\beta])} \quad (9)$$

where c_i' = effective cohesion of the ith layer (kPa); L_i = length of the failure plane incorporated within the ith layer (m); S_i = force produced by matric suction on the unsaturated part of the failure surface (kN m^{-1}); ϕ^b = angle representing the rate of increase in shear strength within the increasing matric suction (degrees); W_i = weight of the ith layer; β = failure-plane angle (degrees from horizontal) ; U_i = hydrostatic-uplift force on the saturated portion of the failure surface (kN m^{-1}); P_i = hydrostatic-confining force due to external water level (kN m^{-1}); α = bank angle (degrees from horizontal); and ϕ' = angle of internal friction (degrees).

The result is a numeric factor of stability defined as either unstable (F_s<1) or stable (F_s>1). An additional classification of conditionally stable (1<F_s<1.3), is also included to account for the variability in the bank structure (Parker et al., 2008). This quantification of stability is a fundamental component of this analysis, effectively giving the researcher unique scales of stability upon which to measure and predict dependencies.

The BSTEM model has the capability of running complex failure analysis of multi-layered bank structures through the utilization of the Toe Erosion Model. This model works by first partitioning the bank into nodes at each soil layer and calculating the boundary shear stress acting on each node using a modification of Equation (1). The soils resistance to the effective boundary shear stress is determined through the application of the submerged jet-test device

(Section 3.4). With these parameters known, erosion rates can be calculated for each node by applying Equation (2).

Since there were time limitations associated with this study, the Toe Erosion component of BSTEM was utilized in an effort to simulate bank failure and determine erosion quantities. To best represent each bank, the cross section with the median F_s for each bank was chosen to represent each site. Bankfull flow durations are reported to last between 1.5 to 11 days annually (Andrews, 1980). However, durations are subject to local stream conditions and can vary drastically between river systems and regions (Hey, 1998). For these reasons, a standardized bankfull flow duration of 2 days was selected for all sites to project erosion and bank geometry changes. The bankfull flow simulation was followed by a sudden drawdown of water surface in an attempt to maximize stress on the bank structure so that a better understanding of the stability of each bank could be accomplished.

3.3 Bank Heterogeneity Characterization

The most integral component of this research entails the detailed characterization of the stream bank heterogeneity. The focus of this endeavor was to denote the spatial location of all erodible and non-erodible components on a two-dimensional coordinate system so that spatial relationships could be achieved. A systematic sampling effort was employed with 0.1 x 0.1 meter grid spacing. This 0.1m spacing was selected to make the resolution as descriptive as possible, while keeping the quantity of points at a reasonable number, so that an accurate measure of the stream bank structure and heterogeneity could be obtained.

These measurements were obtained by first constructing an apparatus with the ability to form to the contours of a stream bank and thereby possessing the capability for standardized grid sampling. A durable tarpaulin with a detailed 0.1m grid containing small holes at the intersections of the grid was employed. The apparatus was pinned to the bank face contour to

capture an accurate spacing of all points measured, effectively transforming the three-dimensional structure into a two-dimensional grid for simplified analysis. A mini penetrometer was applied to probe the bank structure at each point on the grid. If the penetrometer penetrated the surface of the bank, the measurement was classified as soil. If the penetrometer was unable to penetrate the bank surface, further inspection was required to determine if the structure was classified as hardened soil or a non-erodible point (Figure 3 - 1). This data was then converted into binary data for spatial analysis (Section 3.6). A value of '0' was given to erodible points, and a value of '1' was given to resistant, non-erodible points. To limit experimental error, a single user measured all values at every site.

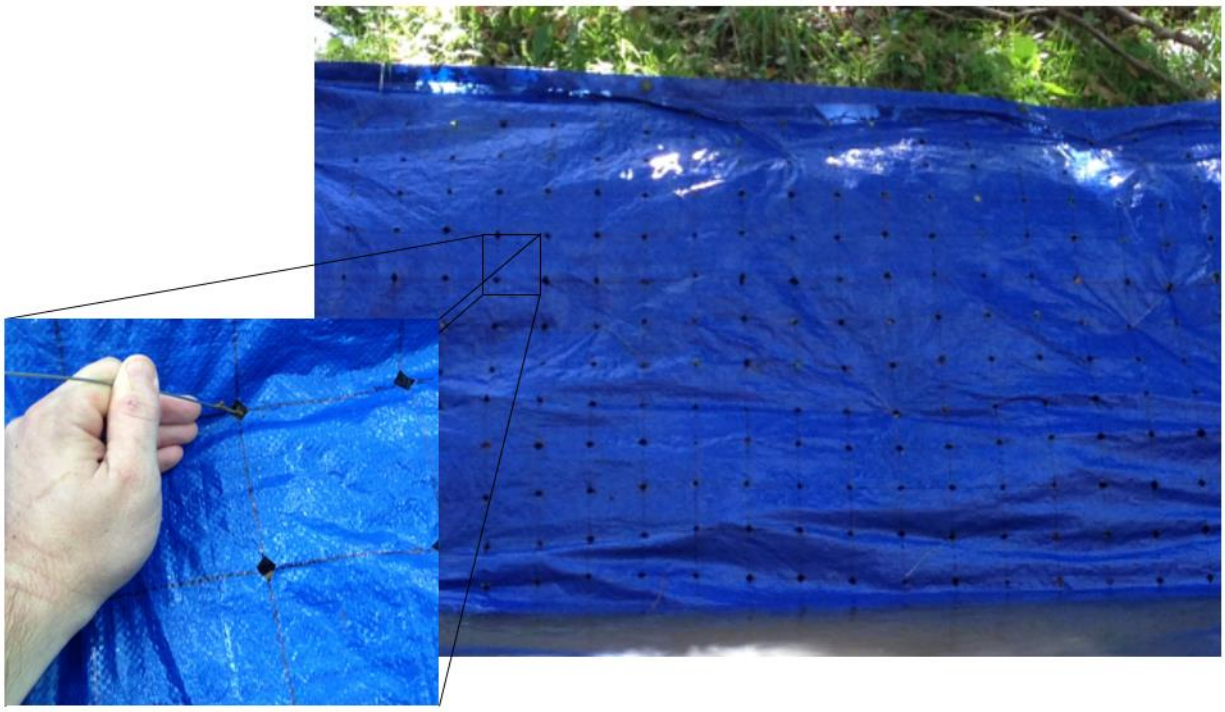

Figure 3 - 1: Streambank Heterogeneity Classification Sampling Effort

.

3.4 In-situ Soil Shear Strength and Erodibility Determination

To quantify the strength of the streambank soil matrix and its susceptibility to erosion, in-situ measurements were necessary. Several methods are available for determining the critical

shear stress and soil erodibility (Clark and Wynn, 2007); however the apparatus selected was the “mini” submerged jet test device. Smaller and lighter than the original version of the submerged jet test device developed by Hanson (1990), the “mini” apparatus allows greater flexibility in testing locations and is easier to transport making it more advantageous for exhaustive field analysis (Al-Madhhachi et al., 2013a). Further, this added convenience does not diminish the accuracy of the test. Al-Madhhachi et al. (2013b) compared the original submerged jet apparatus with the “mini” version in a laboratory setting and found that both devices provided statistically equivalent and accurate results for the erodibility coefficient (k_d), and the critical shear stress (τ_c) of the soil structure.

The “mini” jet test device consists of a base ring, submergence tank, rotatable plate, rotatable nozzle, depth gage, pressure gage, valve, water inlet and outlet, and hoses (Figure 3 - 2). To initiate the test, the base ring is first forced into the soil structure to a depth of approximately 51mm after which the submergence tank is attached, creating a seal with the base ring. The tank filled with water which is delivered to the apparatus by an in-stream pump. The water velocity is regulated through a valve and measured through the pressure gage. The jet of water travels through the 3.18mm nozzle at a constant velocity where it impacts the soil surface, diffuses radially and produces a shear stress along the soil resulting in scour. A point gage is applied in periodic intervals to measure the scour depth throughout the test. These pressure, scour, and time measurements are used to estimate the equilibrium scour depth and consequent critical shear stress and erodibility.

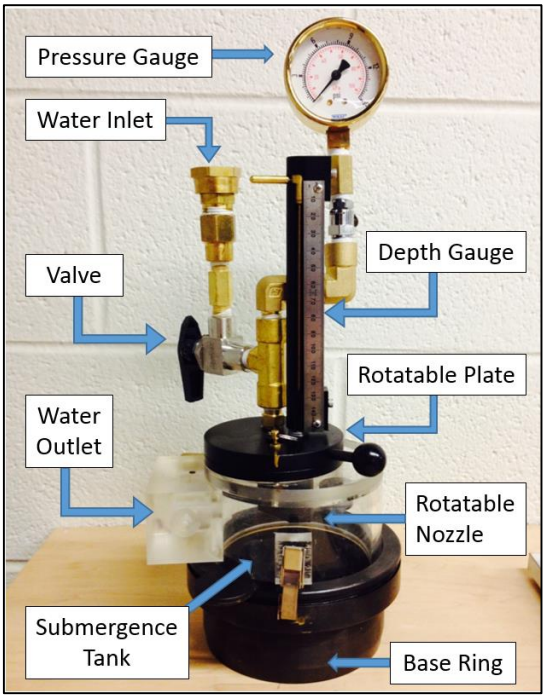

Figure 3 - 2: "Mini" Jet Test Device

The analytical procedure required to translate raw data into quantifiable parameters for the "mini" jet device was first developed by Hanson and Cook (1997, 2004). The methods were developed for the original submerged jet test apparatus; however, the governing principles are consistent for both devices and are based on diffusion principles for scour resulting from a submerged circular jet developed by Stein and Nett (1997). The resulting relationship is a manipulation of Equation (2), defining the erosion rate as equivalent to the rate change in the depth of scour ($\frac{dJ}{dt}$) which is a derivative of the maximum boundary shear stress (Hanson and Cook, 1997):

$$\frac{dJ}{dt} = k_d \left[\frac{\tau_o J_p^2}{J^2} - \tau_c\right], for\ J \geq J_p \quad (10)$$

where J = scour depth (cm); and J_p = potential core length from jet origin (cm).

Initially, the rate of scour is substantial; however, Stein and Nett (1997) determined that it asymptotically approaches zero with time. The depth at which the hydraulic shear stress acting on the soil surface no longer causes a rate change of scour ($\frac{dJ}{dt}$ = 0) is considered to be the equilibrium depth (J_e). The hydraulic shear induced at this point is the critical shear stress of the soil and can be determined by the following equations (Hanson and Cook, 1997):

$$\tau_c = \tau_o \left(\frac{J_p}{J_e}\right)^2 \quad (11)$$

$$\tau_o = C_f \rho U_o^2 \quad (12)$$

$$U_o = C\sqrt{2gh} \quad (13)$$

$$J_p = C_d d_o \quad (14)$$

where C_f = coefficient of friction, 0.00416; ρ = density of water (kg m^{-3}); U_o = velocity of jet at the orifice (cm s^{-1}); C= discharge coefficient; h = pressure head (cm); C_d = diffusion constant, 6.3; and d_o = nozzle diameter, 0.318 cm. In order to insure maximum accuracy within the results, C was calibrated for each “mini” jet apparatus. The procedure and results can be found in Appendix A. Equations (10) and (11) can be integrated into a dimensionless form (Hanson and Cook, 1997):

$$\frac{dJ^*}{dT^*} = \frac{(1 - J^{*2})}{J^{*2}} \quad (15)$$

supported by the following dimensionless scour depth, potential core length, and time equations:

$$J^* = \frac{J}{J_e} \quad (16)$$

$$J_p^* = \frac{J_p}{J_e} \tag{17}$$

$$T^* = \frac{t}{T_r} \tag{18}$$

$$T_r = \frac{J_e}{k_d \tau_c} \tag{19}$$

Integration of Equation (12) yields (Hanson and Cook, 1997):

$$T^* - T_p^* = -J^* + 0.5ln\left(\frac{1+J^*}{1-J^*}\right) + J_p^* - 0.5ln\left(\frac{1+J_p^*}{1-J_p^*}\right) \tag{20}$$

where a iterative spreadsheet routine is next applied using Equations (10) – (20) to determine τ_c and k_d.

Although the equilibrium scour depth (J_e) is used extensively in these calculations, Blaisdell et al. (1981) discovered that the amount of time needed to determine J_e often makes it difficult, and unrealistic, to do so. Estimation of J_e is therefore necessary, through the fitting of scour and time data to a logarithmic-hyperbolic function:

$$A = (f - f_o)^2 - x^2 \tag{21}$$

$$f = log\left(\frac{J}{d_o}\right) - log\left(\frac{U_o t}{d_o}\right) \tag{22}$$

$$f_o = log\left[\frac{J_e}{d_o}\right] \tag{23}$$

$$x = \log\left(\frac{U_o t}{d_o}\right) \tag{24}$$

where A = value for the semi-transverse and semi-conjugate axis of the hyperbola. Microsoft Excel Solver is next applied to solve an iterative process to best fit the values A and f_o and solving for the equilibrium scour depth (J_e).

In an attempt to measure the true structure and variance of the streambank fluvial parameters, a stratified sampling method was applied by dividing the bank into three evenly spaced vertical sections dependent on the height of the bank. Although banks with homogenous soil compositions were selected, this technique allows an insightful look into the changes in fluvial resistance with bank height due to changes in water content, consolidation, and soil properties. The bottom layer was considered the bank toe, while the remaining layers were considered the bank midsection and bank top. An equivalent number of tests were completed within each layer. The objective was to acquire three tests per layer, totaling nine tests per bank. To limit experimental error, a single user measured all values at every site.

3.5 Atterberg Limits Determination

Additional classification of the streambank soil was accomplished through the application of ASTM D4318- Standard Practice for Classification of Soils for Engineering Purposes, also known as Atterberg Limits (ASTM, 1999b). Atterberg limits testing yields the determination of the liquid limit (LL), plastic limit (PL), and plasticity index (PI). In addition to describing several fundamental properties of cohesive soils, these parameters have been found to be correlated with such structural properties as critical shear stress (Smerdon and Beasley, 1961), friction angle (Kanji, 1974), and residual shear strength (Voight,1973; Wesley, 2003). As discussed in Section 2.2, soil properties such as Atterberg Limits vary spatially, sometimes creating a heterogeneous soil structure even in seemingly homogeneous soils (Bull, 1997; El-Ramly et al, 2002; Lacasse and Nadim 1996). For this reason, Atterberg Limit approximations were used to describe the continuity of each bank's soil properties and also utilized in the comparison of streambank sites.

In an effort to remain consistent, soil sampling for Atterberg Limits testing followed the stratified sampling technique utilized in the determination of in-situ shear strength and erodibility

(Section 3.4). However, instead of sampling three locations within each stratified layer, one sample was taken per layer at each bank.

3.6 Spatial Statistics

Classical statistical methods are useful for many earth science applications, however they do not possess the ability to process spatial information (Isaaks and Srivastava, 1989). Therefore, alternative methods must be utilized to derive significant information from spatial data. Three separate methods were applied in the research: nearest-neighbor analysis, join-count statistics, and geostatistical variogram analysis.

3.6.1 Nearest-Neighbor Analysis

One commonly utilized method in spatial investigations is the nearest neighbor analysis. This simply determines the distance between the nearest pairs of data and can be used to find the distance between the nearest k^{th} pair. To quantify the aggregation of the nearest neighbors, Clark and Evans (1954) developed an aggregation index. This index describes the clustering of points through a comparison of the mean nearest neighbor distance between points and expected distances if the points were randomly distributed (Clark and Evans, 1954; Davis, 2002):

$$R = \frac{\bar{d}}{\bar{\delta}} \tag{25}$$

where R = nearest-neighbor index; $\bar{d}$ = observed mean distance between nearest neighbors; $\bar{\delta}$ = expected mean distance between nearest neighbors in a random distribution of equivalent density.

The aggregation index quantifies the distribution of points in a two dimensional plane signifying if clustering is present. The value of R ranges from 0 for a point distribution with

maximum aggregation to 1 for a random point distribution. One prominent problem with nearest neighbor statistics is the presence of edge effects, caused by the test's assumption that the observed point pattern extends infinitely in all directions, leading to an overestimation of R. To compensate for this problem, Donnelly (1978) developed a correction for the boundary effects on a rectangular map through numerical simulation. The aggregation index is a useful tool to define clustering in point pattern data, however does not provide descriptive information about the nature of the structures.

3.6.2 Join-Count Statistics

Another method of describing the spatial structure of binary data is join-count statistics. These are a practical method of determining the magnitude of clustering or dispersion in categorical, binary data and therefore have been utilized in a large spectrum of fields such as ecology (Fortin et al., 2006), genetics (Epperson, 1997), and geography (Hungerford, 1991). Building on nearest-neighbor principles, this type of analysis counts the number of joins between similar and dissimilar cells, providing a measure of the distribution of variation between simple categorical parameters. The data is compiled as white-white (WW), white-black (WB), and black-black (BB) joins with white representing the value 0 and black representing the value 1. The formulas for quantifying the number of joints in a binary polygon grid can be viewed below (Cliff and Ord, 1981):

$$J_{BB} = \frac{1}{2}\sum_i \sum_j \omega_{ij} Y_i Y_j \tag{26}$$

$$J_{BW} = \frac{1}{2}\sum_i \sum_j \omega_{ij} \left(Y_i - Y_j\right)^2 \tag{27}$$

$$J_{WW} = J - J_{BB} - J_{BW} \tag{28}$$

where J_{BB} = number of black-black joins; J_{BW} = number of black-white joins; J_{WW} = number of white-white joins; ω_{ij} = joining weight (1 for joined regions, 0 otherwise) ; Y = value of cell (1 if black and 0 if white).

Additionally, join count methods test for the null hypothesis of no spatial autocorrelation therefore providing a measure of spatial dependence. A Monte Carlo simulation can be applied to determine whether a cell values are distributed binomially, thereby testing the null hypothesis of zero autocorrelation (Cliff and Ord, 1981).

3.6.3 Geostatistical Indicator Variogram Analysis

The final technique used to describe the spatial structure of streambank resistance points was geostatistical variogram analysis. Geostatistics provides the ability to predict spatially dependent probability distributions and describe spatial continuity (Isaaks and Srivastava, 1989). Often used as an interpolation technique (Lacasse and Nadim, 1996), the geostatistical modeling completed in this analysis will include only indicator variogram analysis. Indicator analysis denotes that the data are binary, with values of 0 representing soil and values of 1 signifying non-erodible hard points.

The variogram provides a measure of the spatial structure through a graphical display of the semivariance ($\gamma\ (h)$) between data points at discrete separation distances (lags):

$$\gamma\ (h) = \frac{1}{2N(h)} \sum_{i}^{N(h)} (x_i - x_{i+h})^2 \quad (29)$$

where h is the lag vector spacing; x_i is the value of the measured variable; x_{i+h} is the corresponding value of the measured variable h intervals away; and $N(h)$ is the number of pairs at the interval h. Application of Equation (29) with multiple lag intervals produces an

experimental semivariogram. This method can be employed to analyze directional spatial structure in addition to omnidirectional continuity.

Properly modeling the variogram with proper bounds is completed through a trial an error process. No explicit method exists to select the proper criteria for lag, lag distance, max lag distance; therefore, it must be completed in an arduous manner. An overview of the methods used to properly model the semivariance of each bank structure can be found in Appendix D.

Empirical variograms are often defined by three parameters: the sill, range, and nugget. The sill is the flat region where the semi-variance no longer increases and is often considered to be the field variance. The range is the distance for the semi-variance to reach the sill, identifying the average distance at which points are spatially dependent. The nugget is the discontinuity from the origin to the initial semi-variance value. Theoretically, this quantity should be zero; however, the nugget accounts for measurement error and variations at a smaller scale than measured. It is often portrayed as the relative nugget effect which is the ratio of nugget variance to sill variance, leading to a quantifiable amount of variance attributed to the nugget effect (Isaaks and Srivastava, 1989; Davis, 2002; Rossie et al. 1992). Additionally parameterization of the experimental variogram can be accomplished through the fitting of theoretical variograms; however these models did not sufficiently fit the dataset; therefore, purely descriptive bounds were utilized (Appendix D).

Chapter IV

Results and Discussion

Between July 2013 and November 2013, eighteen streambanks were studied along eight streams in the Ridge and Valley Ecoregion of Eastern Tennessee (Figure 4 - 1). The sites were on 1st to 4th order streams with cohesive streambanks. In an effort to minimize temporal changes to the bank geometry, moisture content, and sediment structure, all parameters were measured at a given site within the short time frame of less than 10 days. The effect of this temporal change could not be completely controlled, however, because moisture content in constantly fluctuating and significant changes occur seasonally. The criterion for selection was that the bank exhibit a uniform slope structure and height along straight reaches for a distance of approximately 10 meters. Uniformity in bank slope and height ensured continuity for each bank, while straight reaches were chosen such that secondary currents could be minimized. The 10 meter reach length standard was not always attainable, however, due to changes in bank contours and uniformity, therefore streambank reach length varied from 7m-10m.

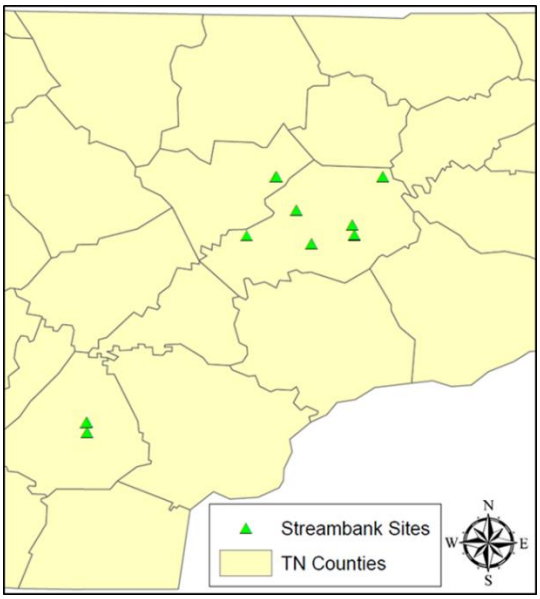

Figure 4 - 1: Streambank Site Locations

Sufficient data were extracted from each site with the expectation of adequately describing the hydrologic properties (Section 4.1), soil structure (Section 4.1), magnitude of stability (Section 4.2), and spatial distribution of non-erodible resistance points (Section 4.3) in an attempt to understand the interactions between the groups (Section 4.4). Three hypotheses were tested within this analysis: (1) streambanks possess a spatial structure and dependence of hard points; (2) streambanks naturally "armor" themselves from fluvial erosion with a combination of hard points and resistive soil; and (3) the stability of the streambank can be predicted by its parameters in addition to its spatial structure.

4.1 Streambank Properties

To properly understand the environment in which the 18 sample sites reside, streambank properties were either measured or remotely estimated. Approximations of drainage area, stream order, and slope were determined from ArcGIS. Using these variables, the bankfull flow rate (Q_{bf}) was estimated using the regional curve developed by McPherson (2011) for the Ridge and Valley Ecoregion of Eastern Tennessee. This approximation was used to calculate the bankfull event stream power (Ω) and stream power per unit area (ω).

Table 4 - 1: Streambank Site Hydrologic Properties

Site	*Drainage Area (km^2)*	*Stream Order*	Q_{bf} *(m^3/s)*	S_v *(m/m)*	*Width (m)*	Ω (Watts)	ω (Watts/m)
Beaver Creek-1	188.5	4	52.8	0.00149	16.8	770.0	45.9
Beaver Creek-2	107.8	4	34.3	0.00200	12.3	673.0	54.5
Beaver Creek-3	107.8	4	34.3	0.00200	12.3	673.0	54.5
Flat Creek-1	95.6	3	31.3	0.00716	19.3	2200.8	114.3
Flat Creek-2	95.6	3	31.3	0.00716	19.3	2200.7	114.3
Hinds Creek-1	96.7	3	31.6	0.00231	14.1	715.3	50.7
Hinds Creek-2	86.0	3	28.9	0.00231	17.5	653.6	37.4
Loves Creek-1	24.6	2	11.0	0.00161	9.9	174.0	17.5
Loves Creek-2	24.6	2	11.0	0.00161	9.9	173.9	17.5
Oostanaula Creek-1	59.3	3	21.7	0.00149	11.3	317.7	28.0
Oostanaula Creek-2	59.4	3	21.7	0.00149	11.3	318.1	28.0
Swan Pond Creek-1	30.9	2	13.1	0.00371	9.3	477.6	51.2
Swan Pond Creek-2	30.7	2	13.1	0.00371	8.8	475.8	53.9
Third Creek-1	33.3	3	13.9	0.00264	8.8	359.7	40.8
Third Creek-2	33.3	3	13.9	0.00264	9.8	359.7	36.7
Third Creek-3	33.3	3	13.9	0.00264	8.8	359.7	40.7
Walker Branch-1	2.1	1	1.6	0.01353	6.8	216.1	32.0
Walker Branch-2	2.1	1	1.6	0.01353	6.8	217.4	32.2

It should be noted that slight under estimations of bankfull flow and subsequent stream power might exist due to limitations of the McPherson (2011) approximation, Equation (6). The curve was developed for the Tennessee Ridge and Valley Ecoregion, which all sites exist within, using several inputs. All sites in this research met the requirements for this regional curve, with the exception that the contributing watersheds development be less than 20%. While several of the sites in this study meet this requirement, a few are located in areas that are significantly more developed. To test this effect, stream widths predicted based on the McPherson's regional curve were compared with those measured in the field. It was determined that the regional curves over predicted the width by 14% on average. This could be due to the weakness of the regional curve, however this may also be an indication of systematic incision throughout the sites. Although the predicted Q_{bf} might not produce values consistent with Andrews (1980) definition of bankfull flow utilized by McPherson (2011), the approximation gives appropriate

standardized effective discharge values for the sites. It is believed that since this estimation of energy within the stream is being used for comprehension of the parameters controlling streambank stability and heterogeneity that this slight inaccuracy is acceptable. That is, the results of this study are not dependent on highly accurate estimations of stream energy. Before designing natural streambanks and assessing for their stability it is suggested that hydrologic measurements be made in the field to more adequately approximate this bankfull event.

Erodibility parameters τ_c and k_d were measured in-situ using the mini submerged jet test apparatus. A total of 9 tests were completed at each site utilizing a random stratified sampling technique when possible. It was not feasible to achieve all 9 measurements at several sites due to extenuating circumstances such as impending storm events and equipment malfunction. One user measured ran all erodibility Critical shear stress results from individual jet tests range from approximately 0.093 Pa to 48.5 Pa, while erodibility varied between 0.095 to 10.5 cm^3/N-s. Within each site these values varied between one and three orders of magnitude. These results are consistent with other researchers studying streambank erosion (Wynn and Mostaghimi, 2006; Hanson and Simon, 2001) and are likely due to variations in moisture conditions and matric suction due to bank height causing localized weakness. Therefore, τ_c and k_d were averaged for each site so that a better understanding of the composite bank properties could be achieved. Each streambank was additionally assigned an erodibility classification developed by Hanson and Simon (2001) to better qualitatively describe the sites and partition them for further analysis. Further classification of the soil properties was accomplished through determination of the Atterberg Limits according to ASTM D4318 (ASTM, 1999b). Three samples were taken from each site, utilizing a stratified technique similar to that used by the in-situ jet testing. Table 4 - 2 provides an overview of the average sediment properties from each bank as well as the standard deviations of the erodibility properties so that the variability in these critical parameters can be better understood.

Table 4 - 2: Streambank Site Sediment Properties

Site	LL_{avg} (%)	PL_{avg} (%)	PI_{avg} (%)	$\tau_{c,avg}$ (Pa)	$\tau_{c,\sigma}$ (Pa)	$K_{d,avg}$ (cm^3/N-s)	$K_{d,\sigma}$ (cm^3/N-s)	Erodibility Class+
Beaver Creek-1	38	18	20	10.5	6.7	0.8	0.8	Resistant
Beaver Creek-2*	47	24	24	1.5	0.9	8.3	6.2	Erodible
Beaver Creek-3	44	23	21	9.2	9.7	1.2	1.0	Moderately Resistant
Flat Creek-1	41	24	18	6.3	6.3	2.3	3.3	Moderately Resistant
Flat Creek-2**	39	22	17	20.4	18.6	1.0	1.5	Resistant
Hinds Creek-1	29	18	10	8.2	9.0	2.6	2.7	Moderately Resistant
Hinds Creek-2	28	18	10	6.2	1.0	1.2	1.0	Moderately Resistant
Loves Creek-1	33	20	13	5.1	4.6	0.8	0.3	Moderately Resistant
Loves Creek-2	32	20	12	12.8	6.5	0.7	0.5	Resistant
Oostanaula Creek-1	35	19	16	15.0	9.6	0.6	0.4	Resistant
Oostanaula Creek-2	37	19	18	9.7	10.8	0.8	0.7	Moderately Resistant
Swan Pond Creek-1	27	17	10	10.4	8.3	0.9	0.7	Resistant
Swan Pond Creek-2	39	20	20	14.0	4.3	0.8	0.5	Resistant
Third Creek-1	32	19	14	11.6	4.2	0.8	0.5	Resistant
Third Creek-2	32	19	13	13.2	4.9	0.8	0.5	Resistant
Third Creek-3	35	17	18	11.6	8.2	1.1	0.6	Resistant
Walker Branch-1**	28	17	11	3.8	4.4	1.4	0.7	Moderately Resistant
Walker Branch-2	29	18	11	1.6	1.5	3.6	2.7	Erodible

Note: For LL, PL, PI n=3 * n = 6 for τ_c, K_d + Based on classes developed by
For τ_c, K_d n=9 unless noted ** n=8 for τ_c, K_d Hanson and Simon (2001)

Individual Atterberg Limits results for each test were plotted on the Unified Soil Classification System plasticity chart (Figure 4 - 2) (Casagrande, 1948). All of the streambank soil samples possess similar attributes of low to medium plastic clays, with a few isolated samples converging on silty behavior. Furthermore, there does not appear to be a distinct difference between those soils located at the top, mid, or toe sections of the bank.

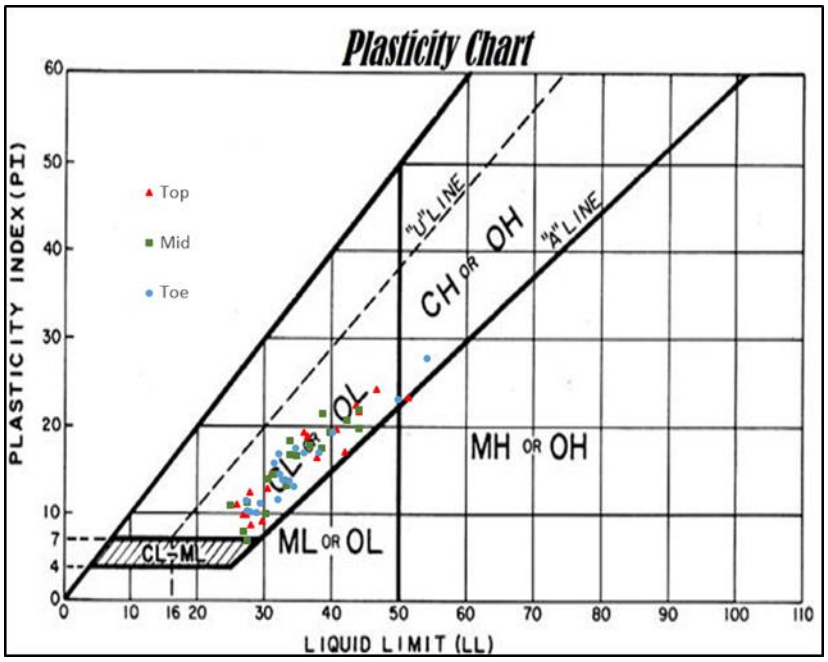

Figure 4 - 2: USCS Plasticity Chart showing Individual Classifications

Differences in soil properties were evaluated using a combination of analysis of variance and non-parametric Mann-Whitney tests. Samples tested with ANOVA must come from normally distributed datasets (Davis, 2002). The Atterberg Limits of soils have been found to be normally distributed in nature (Lacasse and Nadim 1997). Additionally, the fluvial parameters were tested for normality using the Shapiro-Wilk test at p=0.05. All but 3 banks demonstrated a normal distribution for τ_c measurements, leading to the assumption that τ_c values also are derived from normal distributions. However, normality testing for k_d yielded only 6 banks which come from a normal distribution (Appendix B). Therefore, it is assumed that LL, PL, PI, and τ_c display a normal distribution in stream banks and ANOVA is applicable to this dataset; however, k_d must be tested separately using non-parametric estimations. To further ensure accuracy of ANOVA testing, the residuals were tested for normality, of which they passed (p=0.05). The results in Table 4-3 include comparison of parameters between all sites, Hanson and Simon (2001) erodibility classes, and conditioned stability classes (Section 4.2).

Table 4 - 3: Comparison of Soil Parameters

	A	*B*	*C*
	pf>F	pf>F	pf>F
τ_c	<0.0001	<0.0001	0.0017
k_d *	<0.0001	0.0061	0.0106
LL	0.0001	0.7003	0.4565
PL	0.0331	0.4367	0.3288
PI	<0.0001	0.7147	0.5351

A=Between All Sites; B= Between Erodibility Classes;

C = Between Stability Classes; * = tested with Mann-Whitney

When comparing every streambank site, all five variables were found to vary significantly between sites. This result is meaningful, however not unexpected. Significant differences in τ_c and k_d are anticipated between sites due to local conditions and the variety of factors that control them such as moisture content, weathering, and consolidation. Additionally, differences in Atterberg limits were expected due to the number of sites studied, making it unlikely that these values would be equivalent between sites.

Assessing the difference in soil properties between erodibility groups is more descriptive. The erodibility parameters τ_c and k_d were significantly different between groups. This was anticipated because there are inherent divisions in τ_c, and therefore k_d, due to the imposed classification of erodibility groups. The Atterberg Limits, however, appear to be similar between soil erodibility groups.

Similarly, when comparing the conditioned stability classes, significant differences in soil erodibility exist; however, the Atterberg Limits do not display significant differences. The lack of statistical difference in Atterberg limits between erodibility and stability classes, along with the USCS classification (Figure 4 - 2), reinforces the belief that all of the streambank sites have similar soil types. It is likely that the differences in Atterberg Limits between all streambank sites is due to the larger number of groups compared, making it unlikely that the means would be

equivalent between all sites. Therefore, when comparing the means of smaller numbered groups, the Atterberg limits converge on similar values. The fact that erodibility values were statistically different between stability classifications is an intriguing result that appears like a logical division. It is expected that erodibility would differ between stable and unstable banks, with higher τ_c and therefore lower k_d, values helping maintain bank stability. This result is advanced in further discussion in Section 4.2.2

4.2 BSTEM Modeling

The USDA Bank Stability and Toe Erosion Model (BSTEM) was utilized in an attempt to quantify the stability of each streambank site and segregate sites into stability classes. Three cross sectional measurements, and therefore three BSTEM F_s values, were made/calculated at each site to ensure bank continuity (Table 4 - 4). Although several banks appeared to be unstable, BSTEM determined that all sites possessed stable streambanks. This is due to the cohesive strength of clay, and the bank parameters being measured at a moment in time when the bank was not actively failing; therefore, the modified Mohr-Columb F_s relationship predicted that the banks remained statically stable. It was desired, however, to develop a more robust measure of stability and partition banks into classes so that an understanding of what makes streambanks stable could be achieved.

To capture a more accurate depiction of the magnitude of stability, each bank was conditioned using the BSTEM toe erosion component to predict lateral retreat in a sequential fashion. This conditioning of the bank modeled a discrete hydrograph categorized by an immediate rise in the water surface from base flow to bankfull conditions, followed by 48 hours of bankfull flow and the subsequent immediate drawdown of the water surface back to base flow levels. This purposefully simulates the condition stated frequently in literature following large flow events during the recession of the hydrograph when streambank stability is most vulnerable

due to a disproportionately heightened water table causing a force imbalance (ASCE, 1998a; Simon et al., 2000). Additionally, this generates the severe force caused by bankfull events resulting in fluvial scour on the bank face and toe, further decreasing stability. Bankfull delineations for the BSTEM simulation were made by locating the top point of a bank which connects to the flood plain. This definition is consistent with that used by McPherson (2011) in his regional curve study and with those found in literature (Andrews, 1980; Harrelson et al., 1994).Throughout the testing, the water table was kept at a constant 80% bank height level in an attempt to mimic worst case conditions and maintain continuity throughout the tests. The time chosen for the peak flow period was done so as to not over condition the bank profile. This 48 hour duration is on the low end of the bankfull durations determined by Andrews (1980) between 1.5 and 11 days. The purpose of this simulation was to reach or exceed the critical threshold for approximately half the sites.

Table 4 - 4: Derived BSTEM Values

Site	*Mean Static FS*	*Static FS σ*	*Conditioned* F_s	*Max Lateral Retreat (m)*	*Max Eroded Area (m²)*	*Conditioned Stability Category*
Beaver Creek-1	2.3	0.28	1.1	1.7	1.7	Conditionally Stable
Beaver Creek-2	2.6	0.25	0.7	86.4	111.5	Unstable
Beaver Creek-3	7.3	0.78	2.1	2.7	2.4	Stable
Flat Creek-1	1.8	0.47	0.3	42.1	76.6	Unstable
Flat Creek-2	3.9	2.08	2.1	15.7	21.1	Stable
Hinds Creek-1	2.3	0.22	1.2	17.6	26.0	Conditionally Stable
Hinds Creek-2	9.2	1.29	0.6	9.2	6.3	Unstable
Loves Creek-1	14.1	5.34	5.9	0.9	0.4	Stable
Loves Creek-2	7.4	1.11	2.5	0.9	0.3	Stable
Oostanaula Creek-1	9.5	1.79	9.7	0.1	0.0	Stable
Oostanaula Creek-2	2.8	0.40	2.2	7.8	0.6	Stable
Swan Pond Creek-1	3.9	0.90	1.1	3.9	2.1	Conditionally Stable
Swan Pond Creek-2	4.3	1.39	2.1	0.8	0.2	Stable
Third Creek-1	4.4	1.75	1.1	5.6	1.9	Conditionally Stable
Third Creek-2	4.9	2.43	1.3	2.7	1.0	Stable
Third Creek-3	4.4	0.13	1.6	1.0	0.3	Stable
Walker Branch-1	7.2	0.88	0.5	30.7	42.1	Unstable
Walker Branch-2	3.0	0.70	0.1	99.7	115.6	Unstable

Consistent with Thorne (1982), bank dynamics occur in a cyclical fashion. As they fail, they re-stabilize before additional failure. The hourly BSTEM simulation realized this phenomena; however, BSTEM does not account for failed mass at the toe reinforcing the bank from hydraulic scour. Therefore the eroded masses and lateral retreat quantities can be greatly exaggerated in banks with fragile parameters. Additionally, several of the bankfull simulations might overcompensate the amount of instability and erosion due to severe incision causing an elevated bankfull delineation. Finally, BSTEM predicts scour based on flow level and slope, not taking into consideration resistance, and therefore reduction of velocity, caused by vegetation and other interactions. A combination of these factors makes BSTEM simulations sensitive; however, the modeled bankfull event still provides further insight into the susceptibility of each streambank to failure. Also, analyzing the failure predictions and stability measures after a bankfull event followed by sudden drawdown is more indicative of the actual stability of the bank than a static approximation. Figure 4 - 3 includes the changes in F_s from its original state to the conditioned F_s in addition to the predicted maximum lateral retreat.

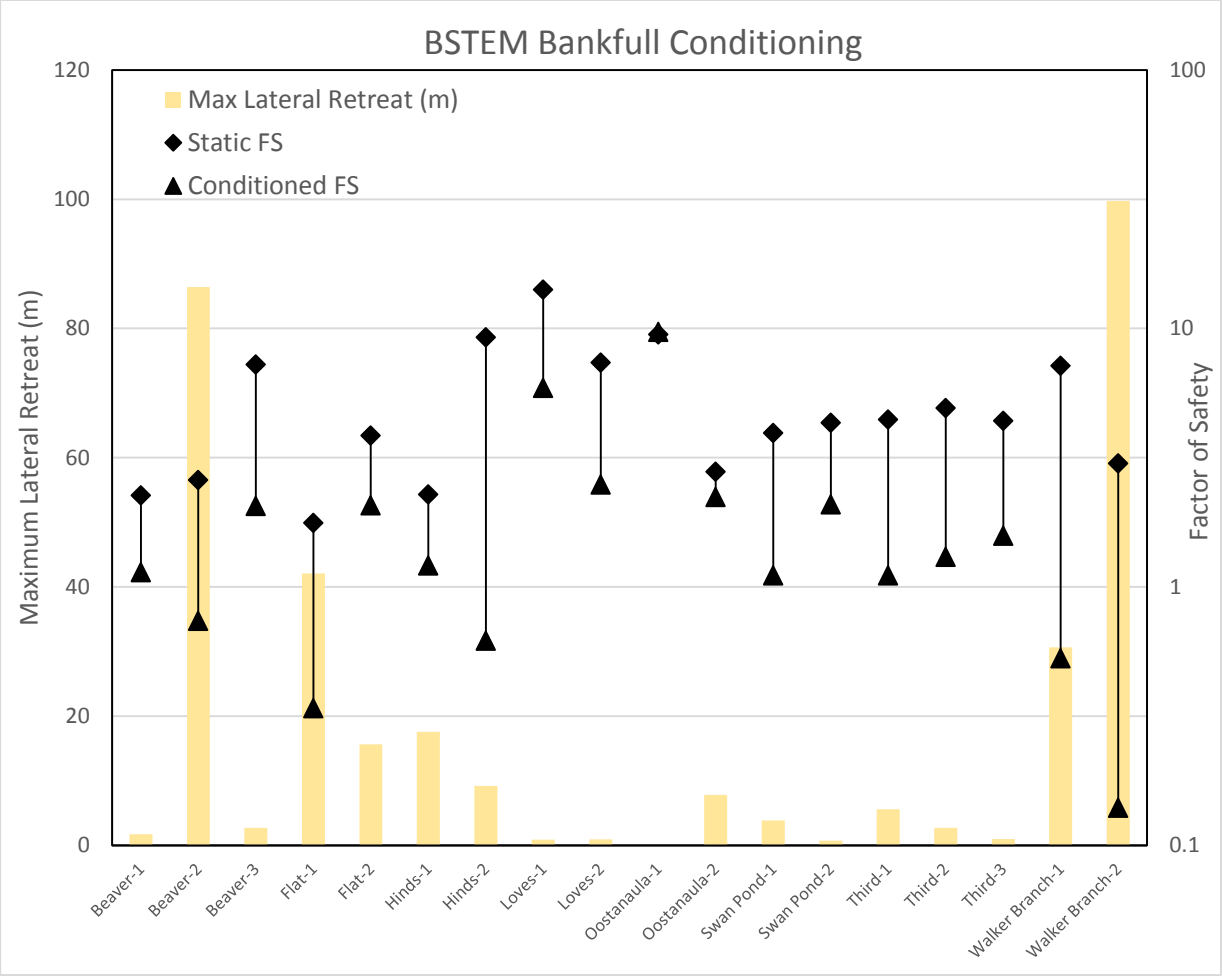

Figure 4 - 3: BSTEM Bankfull Modeling Results

As mentioned previously, several banks exhibit lateral retreat in excess of what is reasonable due to the nature of the BSTEM application. The important conclusion from this analysis is the conditioned F_s values and their subsequent stability categories. Figure 4 - 3 shows that although banks with the most sensitive soil structures are likely to result in instability, this delicacy is not a prerequisite for significant reduction in the F_s. All but two of the sites are conditioned to F_s<3, with a large proportion converging on instability. Further bankfull conditioning was considered; however, abandoned due to the susceptibility of a few banks and the desire for a concentration of banks in the conditionally stable range so that threshold bank conditions could be compared.

4.3 Spatial Correlation of Resistance Points

It has been proposed that a spatial structure of resistant, non-erodible, hard points exists on the face on natural streambanks. To test this hypothesis and determine the extent of the heterogeneous structure and spatial dependence, three methods have been utilized: (1) nearest-neighbor analysis to determine aggregation of points (Section 4.3.1), (2) join count statistics to determine spatial autocorrelation and further quantification of clustering (Section 4.3.2), and (3) semi-variogram analysis to describe the spatial structure with respect to distance (Section 4.3.3).

4.3.1 Nearest-Neighbor Relationships

Nearest neighbor analysis is a traditional technique used to characterize spatial data. To describe the spatial distribution of non-erodible hard points, the Clark and Evans (1954) aggregation index (R) was utilized accounting for boundary effects with Donnelly (1978) method. The aggregation index compares the average distance between the nearest neighbors of similar values with a theoretical expected distance. The result is an R index ranging from a value of 1 for a random distribution of points to 0 for a complete cluster where all points are separated by a null distance (Davis, 2002).

Table 4 - 5: Summary of Range of R Indexes

	Minimum	***Maximum***	***Median***	***Average***
R	0.43	0.89	0.61	0.64

A Monte-Carlo simulation was utilized to test the significance of these results by comparing the measured distribution to 1000 simulations of random Poisson point process distribution of the same density. The null hypothesis is that the points are spatially random and the alternative hypothesis tests is the points are of a regular, ordered point pattern. All banks provided significant results to $p<0.005$, implying a spatial clustering of resistance points. The

range in values suggests that all of the streambank sites sampled possess some degree of aggregation, without substantial singular clustering (Table 4 - 5). This result is expected because objects, such as root and rock masses, are similar at close distances however diminish their relation with distance. Itemized values for each site can be seen in Table 4 - 6 shown in order from what is considered to be most clustered to least clustered:

Table 4 - 6: Aggregation Index (*R*) per Nearest-Neighbor Analysis (0=complete clustering, 1=spatially random)

Site	*R*
Beaver Creek-2	0.43
Flat Creek-1	0.5
Hinds Creek-2	0.52
Beaver Creek-3	0.53
Walker Branch-1	0.53
Hinds Creek-1	0.54
Loves Creek-1	0.55
Oostanaula Creek-2	0.58
Oostanaula Creek-1	0.6
Loves Creek-2	0.61
Flat Creek-2	0.7
Swan Pond Creek-1	0.7
Walker Branch-2	0.71
Beaver Creek-1	0.73
Swan Pond Creek-2	0.75
Third Creek-2	0.78
Third Creek-3	0.87
Third Creek-1	0.89

While R provides a coarse estimate of clustering in the streambanks, a critique of this method is its dependence on the number of points for each individual analysis. For example, Loves Creek-Bank 2 (Appendix E) appears to be strongly aggregated; however, when comparing with banks such as Beaver-2 and Loves-1, R implies that Loves-2 is less clustered. Upon visual inspection this does not seem like an adequate comparison. Due to the nature of the nearest neighbor calculations, the more points within a bank leads to a larger density of

points and therefore smaller expected nearest-neighbor distance. This result contributes to a skew in the quantitative analysis of streambank structures with minimal or maximal resistant points. This circumstance repeats itself throughout the analysis depending on the overall density of hard points along the streambank as seen in Figure 4 - 4.Therefore, these results are useful for the qualitative reasoning that the streambanks are moderately clustered, however, leave more to be desired.

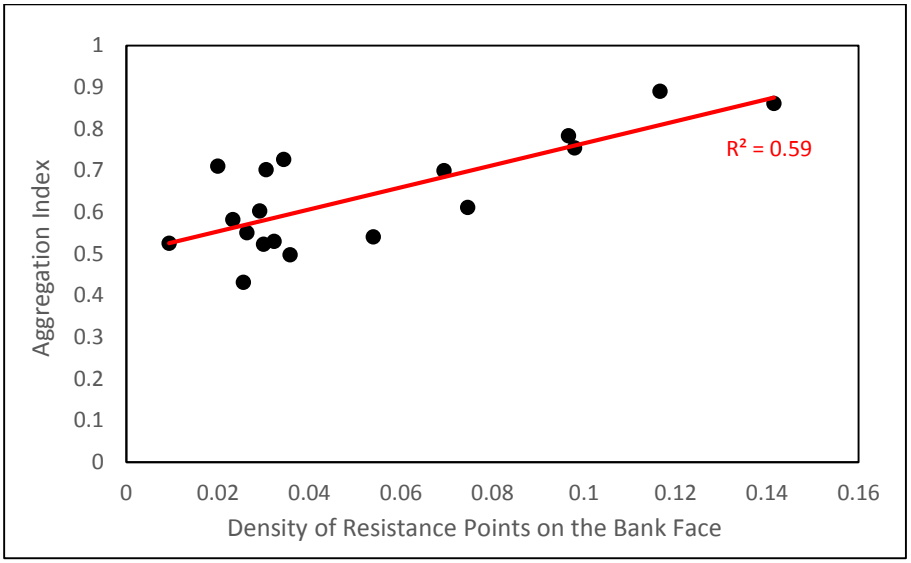

Figure 4 - 4: Comparison of the Aggregation Index with Overall Density of Points

Further investigation into the clustering of resistance points along the bank face was accomplished by analyzing the mean distance among the five nearest neighbors of each non-erodible component. A significant (p=0.01) positive linear relationship exists between the mean k^{th} nearest-neighbor distance and the k^{th} nearest neighbor for all sites (Figure 4 - 5). The slope of this relationship allows simple quantification of the rate change in mean distance between neighbors. This provides an improved understanding of the cluster density of the resistance points on the streambanks.

Table 4 - 7: Nearest Neighbor Analysis

Site	*Mean Distance of Nearest Neighbor (m)*	*Mean Distance of 2nd Nearest Neighbor (m)*	*Mean Distance of 3rd Nearest Neighbor (m)*	*Mean Distance of 4th Nearest Neighbor (m)*	*Mean Distance of 5th Nearest Neighbor (m)*	*NN-Slope*
Beaver Creek-1	0.21	0.31	0.46	0.53	0.60	0.0988
Beaver Creek-2	0.16	0.31	0.83	0.93	1.05	0.2409
Beaver Creek-3	0.17	0.34	0.45	0.58	0.66	0.1237
Flat Creek-1	0.14	0.24	0.32	0.38	0.45	0.0768
Flat Creek-2	0.21	0.33	0.50	0.61	0.70	0.1254
Hinds Creek-1	0.12	0.17	0.29	0.33	0.38	0.0683
Hinds Creek-2	0.16	0.27	0.34	0.38	0.43	0.0648
Loves Creek-1	0.19	0.42	0.51	0.61	0.75	0.1305
Loves Creek-2	0.12	0.16	0.20	0.25	0.32	0.0496
Oostanaula Creek-1	0.20	0.27	0.41	0.53	0.71	0.1289
Oostanaula Creek-2	0.21	0.40	0.56	0.69	0.81	0.1491
Swan Pond Creek-1	0.14	0.21	0.28	0.36	0.41	0.0695
Swan Pond Creek-2	0.13	0.19	0.27	0.32	0.37	0.0621
Third Creek-1	0.14	0.19	0.24	0.28	0.33	0.0493
Third Creek-2	0.13	0.17	0.21	0.25	0.29	0.0400
Third Creek-3	0.12	0.16	0.20	0.25	0.29	0.0428
Walker Branch-1	0.32	0.70	1.27	1.55	2.45	0.5111
Walker Branch-2	0.28	0.40	0.63	0.77	0.86	0.1531

Table 4-7 provides more insightful estimates of hard point cluster density along the bank face compared to the R index. Table 4-8 offers a summary of the values. The slope rate of change (NN-Slope) models the intensity of clustering on the bank and is similar to variogram modeling; however, instead of comparing points at a predetermined distance this method finds the average distance at the k^{th} nearest pair. Large NN-slopes indicate a greater rate of change in distance between nearest neighbors, signifying sparser clustering compared to bank sites with smaller NN-slopes. The nearest neighbor analysis provides insight into the nature of streambank structures. It has been determined through the aggregation index that non-erodible hard points tend to cluster along the face of streambanks and the k^{th} nearest neighbor analysis has quantified the degree of clustering for each site.

Table 4 - 8: Summary of NN-Slope Values

	Minimum	*Maximum*	*Median*	*Average*
NN-Slope	0.040	0.511	0.088	0.121

4.3.2 Join Count Statistics

Join-count statistics are built on nearest-neighbor principles by tallying the number of joins between similar and dissimilar cells which contact each other. The queens method of join-counting was used so that he joins in every direction were accounted for. The data is compiled as white-white (WW), white-black (WB), and black-black (BB) joins with white representing the value 0 (soil) and black representing the value 1 (non-erodible structure). Additionally, join count methods test for the null hypothesis of no spatial autocorrelation therefore providing a measure of spatial dependence. By utilizing a Monte-Carlo simulation with 1000 simulations to compare measured joins to a sequence of spatially random joins, significance can be achieved.

Table 4 - 9: Join Count Statistics

Site	*WW*	*BB*	*WB*	*% BB*	*%BW*
Beaver Creek-1	6442	42	364	0.61%	5.32%
Beaver Creek-2	3008	11	148	0.35%	4.67%
Beaver Creek-3	2803	12	166	0.40%	5.57%
Flat Creek-1	12229	122	656	0.94%	5.04%
Flat Creek-2	13210	54	730	0.39%	5.22%
Hinds Creek-1	6961	133	548	1.74%	7.17%
Hinds Creek-2	7248	80	314	1.05%	4.11%
Loves Creek-1	3910	19	140	0.47%	3.44%
Loves Creek-2	4332	197	334	4.05%	6.87%
Oostanaula Creek-1	4226	25	215	0.56%	4.81%
Oostanaula Creek-2	6553	20	275	0.29%	4.02%
Swan Pond Creek-1	6469	130	646	1.79%	8.92%
Swan Pond Creek-2	3072	106	494	2.89%	13.45%
Third Creek-1	5544	289	1015	4.22%	14.82%
Third Creek-2	5872	321	655	4.69%	9.56%
Third Creek-3	3749	277	837	5.70%	17.21%
Walker Branch-1	5945	5	104	0.08%	1.72%
Walker Branch-2	6610	14	224	0.20%	3.27%

The Monte-Carlo simulations for all banks yielded the result that the spacing of non-erodible points is not spatially random ($p<0.001$). Table 4 - 9 includes the raw data from the analysis, as well as the percentages of each descriptive join. The number of BB joins displays the amount of dense clusters, signifying continuous hard points or large aggregates such as embedded tree roots or boulders. The number of BW joins represents the heterogeneity and variance of the structure, showing discrete hard points locations or diverse composite bank structure. This result helps continue to develop a descriptive representation of the distribution of non-erodible structures on streambanks, and will help to build relationships between the heterogeneous structure of the bank and contributing parameters.

4.3.3 Semi-Variogram Analysis

Previous methods herein have successfully determined that clustering of non-erodible points occurs naturally along streambanks. These methods have quantified the magnitude of this clustering; however, did not have the capacity to account for their spatial relationship with each other. This was accomplished with indicator semi-variogram analysis.

Analysis of the spatial structure through the investigation of the semi-variogram is a robust tool common in many geospatial fields. This study utilized indicator variogram modeling to describe the distribution of non-erodible hard points along streambank sites to build on previous analysis so that a more complete understanding of spatial structure on streambanks could be understood. Empirical variograms are often defined by three parameters: the sill, range, and nugget. The unknown variance is often portrayed as the relative nugget effect, which is the ratio of nugget variance to sill variance, leading to a quantifiable amount of variance attributed to the nugget effect (Isaaks and Srivastava, 1989; Davis, 2002; Rossie et al. 1992).

A comparison of each site yielded semi-variance values spanning several orders of magnitude due to differences in the overall density of resistance points. Consequently, it was necessary to standardize each variogram by dividing the semi-variance by the field variance to

construct meaningful comparisons (Rossie et al. 1992). Theoretical models were insufficient in describing the data due to noisy and non-traditional structures (Appendix D), therefore the straightforward estimations of the variogram structure including the sill (field variance), range, and nugget were derived (Table 4 - 10).

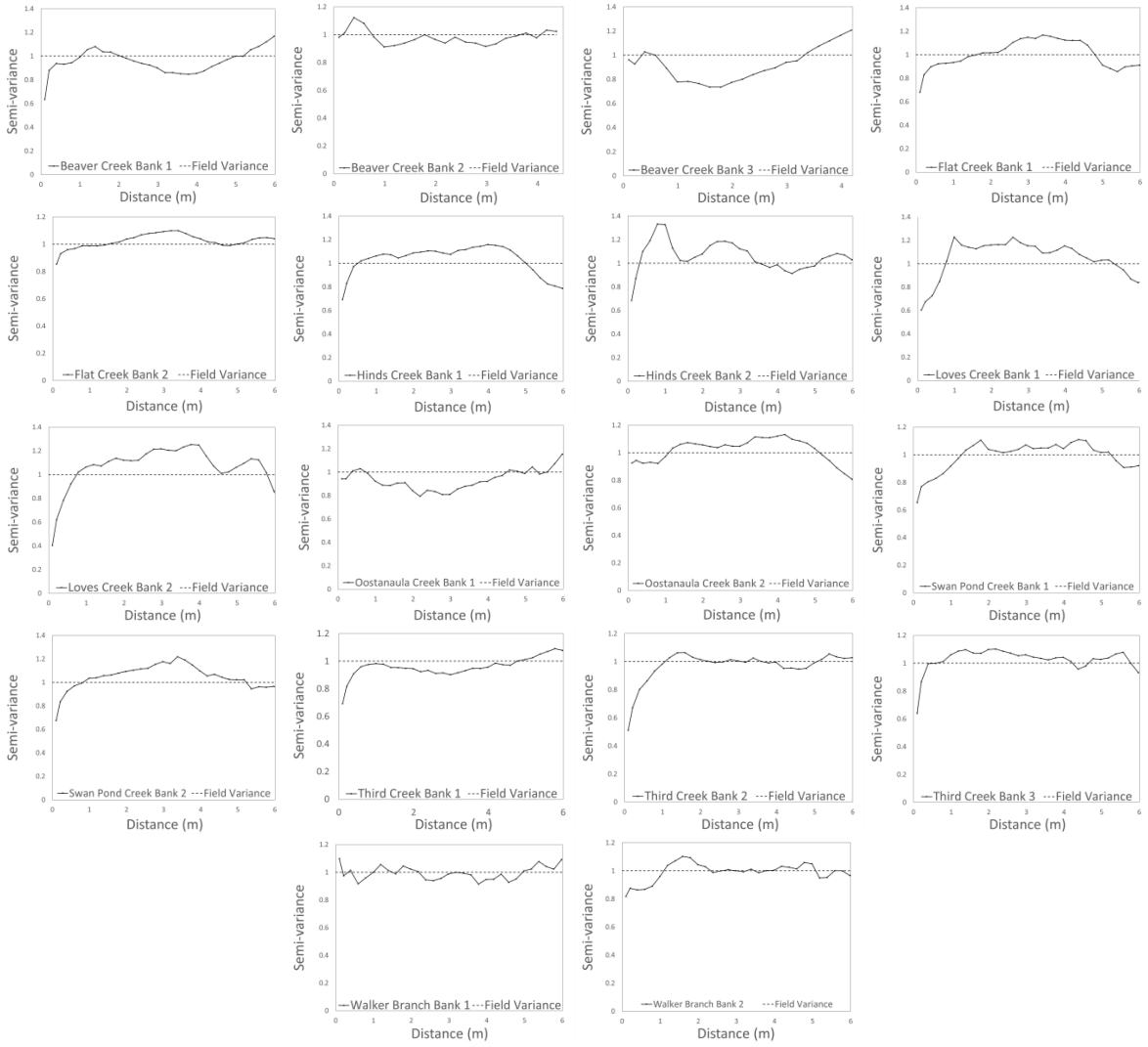

Figure 4 - 5: Standardized Empirical Semi-Variograms

Figure 4 - 5 displays the standardized empirical semivariograms for all sites, including the field variance acting as the sill. At first glance it is evident that the nature of these variograms is relatively variable. This is because the structure of the indicator variogram is

strongly influenced by clustering of data and the relationships between those clusters (Isaaks and Srivasava, 1989; Rossi et al. 1992). Additionally, the noisy structures are due to the resolution of the data. Conflicting prior analysis suggesting all banks possess spatial dependency, variography indicated that several banks do not exhibit strong spatial structure. While this does not exclude the determination that clusters of non-erodible points naturally form along the bank face, it does mean that these clusters are not always spatially dependent on each other. This can be visualized by a pure nugget effect in which the semivariance does not converge on the sill, rather maintains equivalent semi-variance (Rossi et al., 1992). This behavior was quantified by the relative nugget effect (Table 4 - 10) and a cutoff percentage was applied considering banks with greater than 80% nugget effect to possess no spatial structure. This result was confirmed with visual inspection of the variograms. The respective nuggets for each site had a tremendous effect on the structure of the variogram, with a minimum effect of 40%. This is likely due to the resolution of the data, suggesting that the spatial dependence exists at smaller scales than measured. The objective of this study was not to determine the spatial dependence of resistance points at the micro-scale, rather the bank-scale. These non-erodible hard points were measured at decimeter intervals, which according to Croft et al. (2013) is appropriate for the surface roughness at the scale of the river channel. Therefore, the inflated nugget values were deemed acceptable.

Although around 40% of the streambanks do not possess a strong spatial structure, the remaining 60% of banks display a distinct spatial dependence representing the interactions between clustered non-erodible hard points. Table 4 - 10 shows the values of each variogram parameter. The sill is equivalent to the field variance and the range is the distance to which that field variance is reached, often regarded as the distance at which spatial dependence exists between points or clusters. Many variograms peaked within a short distance above the sill, suggesting a slightly larger distance of spatial dependence that the range derives. The

remaining area of semivariance above the sill represents regions in which the variance is greater than the field variance, such as densely spaced non-erodible points.

Table 4 - 10: Semi-Variogram Parameter Summary

Site	*Sill*	*Range (m)*	*Nugget*	*Relative Nugget Effect*	*Spatial Structure?*
Beaver Creek-1	0.033	1.020	0.021	63%	Yes
Beaver Creek-2	0.025	0.165	0.025	98%	No
Beaver Creek-3	0.031	0.343	0.030	96%	No
Flat Creek-1	0.035	1.607	0.023	68%	Yes
Flat Creek-2	0.030	1.494	0.025	85%	No
Hinds Creek-1	0.051	0.509	0.035	69%	Yes
Hinds Creek-2	0.029	0.509	0.020	69%	Yes
Loves Creek-1	0.026	0.763	0.015	60%	Yes
Loves Creek-2	0.069	0.747	0.028	40%	Yes
Oostanaula Creek-1	0.028	0.366	0.027	94%	No
Oostanaula Creek-2	0.023	1.080	0.021	93%	No
Swan Pond Creek-1	0.065	0.819	0.042	65%	Yes
Swan Pond Creek-2	0.088	0.819	0.060	67%	Yes
Third Creek-1	0.103	4.776	0.071	69%	Yes
Third Creek-2	0.087	1.066	0.045	51%	Yes
Third Creek-3	0.122	0.614	0.078	64%	Yes
Walker Branch-1	0.009	0.000	0.010	110%	No
Walker Branch-2	0.020	1.093	0.016	82%	No

Although it has previously been determined that all streambank sites possess clustering of non-erodible points along the bank face, the indicator variogram analysis further isolates the bank which exhibit significant, spatially dependent, clusters interacting with each other. Upon review of the spatially dependent banks, all but one bank possess a nearest-neighbor slope (Section 4.3.1) less than 0.1 m/neighbor. Conversely, all banks which are not spatially dependent possess nearest-neighbor slope > 0.1 m/neighbor. This suggests that the spatial structure of these banks are dependent on dense clustering of non-erodible hard points.

Further investigation into the variograms which indicate significant spatial structure provides insight into the personality of these arrangements. Over half of the spatially dependent banks have periodic variogram structure, possessing local maxima and wave-like configurations. These spatially isolated maxima are clustered resistance points along the bank face. The distances between local maxima and sinuous regions were measured and found to be between 0.39 and 4 meters with a mean distance of 1.4 meters and a standard deviation of 0.84 meters (Table 4 - 11). This result does not serve more than anecdotal evidence of the periodic structure and relationship between clusters; however, coincidentally the average distance between sinuous patterns is similar to the average distance of the range for all points, approximately 1 meter. This observation leads to the assumption that certain streambanks possess non-erodible structures which occur in an oscillating fashion, in this case around every meter of reach length. What controls these patterns is yet to be determined. It is believed that this phenomenon is partially random, however the aggregate structure of the bank and the driving force controlling its stability might also be influential. The values presented in Table 4 - 11, along with the range distances may provide insight into the optimal spacing of cluster along the streambank. This result could potentially be used by designers and practitioners in natural channel design and stability analysis; however further research must be conducted.

Table 4 - 11: Description of Sinuous Variogram Assemblies

Site	*Distance Between Sinuous Structures (m)*				*Average (m)*
Beaver-1	1.00	3.99	-	-	2.49
Flat-1	1.20	1.20	-	-	1.20
Hinds-1	1.19	1.60	-	-	1.40
Hinds-2	1.59	3.20	-	-	2.39
Loves-1	1.59	1.40	1.20	-	1.40
Loves-2	0.69	0.91	0.99	1.40	1.00
SwanPond-1	1.20	0.80	0.60	0.80	0.85

4.4 Interactions between Non-Erodible Structures and Site Parameters

While the previous sections have provided insight into the properties, stability dependencies, and spatial structures of non-erodible hard points along the studied streambanks, a more comprehensive understanding of the natural interactions between these parameters was desired so that substantive relationships can be derived. An exploratory analysis using multivariate analysis was completed to develop conceptual relationships for streambank clustering of non-erodible hard points and bank stability.

4.4.1 Multiple Linear Regression

An initial investigation of all streambanks was completed using stepwise multiple linear regression to determine the influence of soil and stream characteristics on the aggregation of non-erodible distributions. Table 4 - 12 shows the significant linear relationships ($p < 0.1$), all of which were tested for multicollinearity and adequacy of residuals being normally distributed, not autocorrelated, and homoscedastic. The independent variables chosen for these models included all streambank soil (τ_c, $\tau_{c,\sigma}$, k_d, $k_{d,\sigma}$, PL, LL,PI) and hydrologic properties (Q_{bf}, Ω, ω). Strong relationships obviously exist between the respective cluster statistics, therefore these were omitted from analysis.

Table 4 - 12 : Significant Regression Relationships for Non-Erodible Points

			Relationship	*p – value*	R^2_{adj}
(a)	***HP-Variance***	=	$0.02759+0.00608\tau_c - 0.00541\ \tau_{c,\sigma}$	0.028	0.315
(b)	**% BB**	=	$0.00541 + 0.00351\ \tau_c^* - 0.00330\ \tau_{c,\sigma}$	0.014	0.361
(c)	**% BW**	=	$0.3759+0.00776\tau_c - 0.00630\ \tau_{c,\sigma}$	0.031	0.288
(d)	**NN-Slope**	=	$0.21901-0.01087\ \tau_c$	0.058	0.158

HP-Variance = field variance of non-erodible points; % **BB** = % of black-black joins; **% BW** = % of black-white joins; **NN-Slope** = rate change of density between nearest neighbors; τ_c = average soil critical shear strength for each site (Pa); $\tau_{c,\sigma}$ = standard deviation of critical shear strength at each site(Pa);

All contributing parameters are significant to model at p=0.1; a * represents variable significance of p=0.111

Four primary measures of non-erodible clustering converged on statistically significant solutions ($p < 0.1$). The %BB statistic converged on a similar solution, however contained an insignificant variable in the model (τ_c, $p=0.111$). Although statistically insignificant, the relationship mimics the others and therefore has been left in the table for circumstantial comparisons. A common trend emerges from the equations, suggesting that the formation of clustering along the bank face is proportional to the resistant strength of the composite soil profile, accounting for 16 - 36% of the variance. The equations consistently suggest that as the average critical shear strength increases, the density and quantity of resist structures also increases. The reason for this correlation could be due to a number of factors. It is likely that one explanation is the presence of large roots has been found to increase the strength of the soil (Simon and Collison, 2002; Wynn and Mostaghimi, 2006). Not all hard points surveyed were of ecological origin; however, this may account for a sizeable amount of the variance. Likewise, as critical shear deviations increase along the streambank the amount of clustering and total variance in hard points decreases. This may provide further proof of a fundamental interaction between soil and non-soil heterogeneity; however, is most likely resultant of the naturally larger τ_c values having inherently more deviation about the mean due to their inflated value. Regardless of which, this result shows the propensity for τ_c and non-erodible structures to work in coordination to increase streambank resistance.

4.4.2 Discriminant Analysis

Additional exploration into the processes controlling streambank structures and stability was performed using discriminant analysis. Discriminate analysis is similar to other multivariate techniques except the dependent variable is categorical, making it useful to determine the parameters which influence the division of class based groups. Stepwise analysis was first utilized in order to determine which discriminating criterion significantly affect the classification of stability, erodibility, and spatial structure dependence. Variable entry and maintenance within

the model was dependent of a having a $p < 0.1$. The result of which produced the explanatory variables for each respective classification. Following the initial stepwise procedure, the discriminative strength of the derived variables was tested using non-parametric discriminate analysis and examining the cross validation error rate.

Table 4 - 13: Discriminate Analysis of Streambank Classifications

Classification	*Discriminate Variables*		*Error Estimates*		
Stability	τ_c	(λ= 0.428, p =0.0017)	*Unstable*	*Conditionally Stable*	*Stable*
	ω	(λ= 0.284, p =0.0011)	20%	0%	56%
	PL	(λ= 0.186, p =0.0007)			
Spatial Structure	NN-Slope	(λ=0.615,p=0.006	*Spatial Structure*	*No Spatial Structure*	
	LL	(λ= 0.507, p =0.0062)	0%	43%	
Erodibility	HPD	(λ=0.570,p=0.015)	*Erodible*	*Moderately Resistant*	*Resistant*
			50%	100%	33%

ω= unit stream power (Watts/m); HPD = density of non-erodible points on the bank face; λ = Wilks' Lamba

All three classification groups successfully converged on statistically significant discriminates. The discriminate function for indicating spatial structure performed the best, effectively accounting for the presence of spatial structure without error. The forty-three percent error attributed to misclassification of no spatial structure shows the delicacy of the spatial structure to cluster density, i.e. NN-slope. Discrimination of stability groups incorrectly classified one unstable bank as conditionally stable. However, the remaining error on fifty-six percent misclassification of stability is subject to debate. While BSTEM was used to condition the banks into three unique categories based on the stability, the classifications "Conditionally Stable" and "Stable" are in essence the same thing, stable, as both have a F_s>1. The conditionally stable classification was segregated due to having an intermediate factor of safety in an attempt to define the critical threshold of stability condition; however this classification has merely been provided by BSTEM to account for variability (Parker et al., 2008) therefore does not necessarily denote the critical threshold. For the streambank sites provided, this discriminant analysis

seems to agree with the rudimentary definition of stability provide by the F_s, displayed by 100% predictive accuracy on all banks with a conditioned F_s>1. Perhaps what the BSTEM conditioning accomplished was the isolation of banks which are immediately unstable. A distinct division of properties exists between banks considered unstable and those deemed stable. Additionally, building on the ANOVA test on sediment properties between banks and classes (Table 4 - 3), Turkey's HSD Means separation test confirmed the statistical difference between the unstable classification and the stable counterparts. Furthermore, statistical similarities between conditionally stable and stable banks were implied due to the failure to reject the null hypothesis of equivalent means at α =0.05

Segregation between the critical shear stress of stability classifications may partially due to BSTEM conditioning, however is more likely indicative of the factors which cause bank stability in the first place. The average values for τ_c are much larger in the conditionally stable and stable banks, while all unstable banks possess smaller τ_c values (Figure 4 – 6). The range in τ_c for stable banks suggests that there are conditions other than soil strength alone contributing to the stability of the streambank.

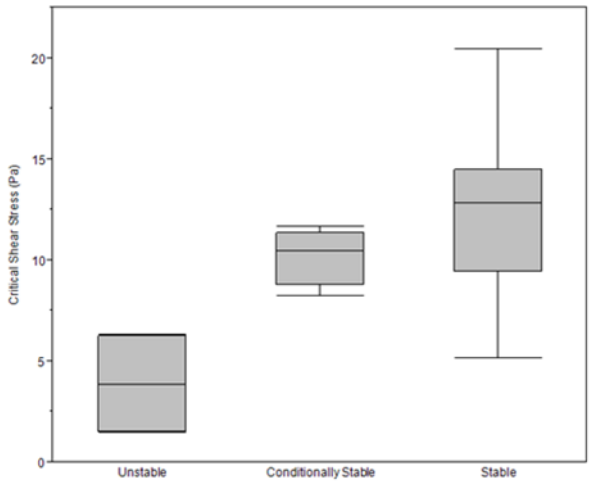

Figure 4 - 6: Mean Critical Shear Stress Distribution for Stability Classes

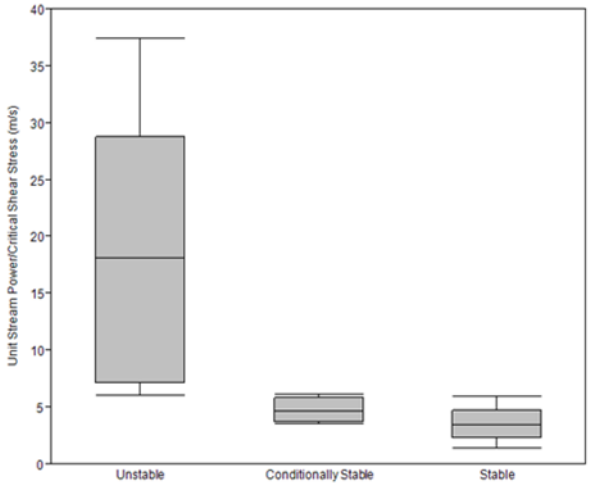

Figure 4 - 7: Excess Velocity Distribution for Stability Classes

A separate variable was developed to quantify the ratio of driving forces (ω) to resisting forces (τ_c). This new relationship (ω/τ_c) represents the amount of excess energy acting on the bank during bankfull flow events caused by a disproportionate relationship of stream power with soil resistance. Dimensionally, this ratio condenses to be equivalent to m/s, therefore has been named the excess velocity. Although comparing small sample sizes, this distinct division in the distribution of excess velocity reveals that it is a driving component of streambank instability.

4.5 Additional Insight into Streambank Stability

Due to previous findings suggesting minimal differences between conditionally stable and stable streambanks, further predictive capabilities were assessed by using modified relationships. This meant simply removing the banks classified to be unstable from the analysis so that stronger functional relationships could be derived for explanatory and possible predictive purposes. Using knowledge of interactions between these variables obtained in previous analysis, multiple linear regression was used.

Table 4 - 14: Stable Regression Relationships

			Relationship	***p - value***	R^2_{adj}
(e)	**BH**	=	0.83253+0.11453 $\tau_{c,\sigma}$	0.0017	0.570
(f)	τ_c	=	9.16001+0.00442Ω	0.0208	0.343
(g)	$\tau_{c,\sigma}$	=	2.35850+0.00536Ω+30.1579**NN-Slope**	0.0008	0.708
(h)	Ω	=	(-)1233.5671 +56.76591τ_c+646.82692**BH**	0.0001	0.800

BH = bank height measured from base of toe (m) **NN-Slope** = rate change of density between nearest neighbors;
τ_c =average soil critical shear strength for each site (Pa); $\tau_{c,\sigma}$ = standard deviation of critical shear strength at each site(Pa);
Ω = Bankfull Stream Power (Watts); **All contributing variables are significant to p=0.1**

Comparing only the banks considered to be stable yields a new set of relationships for the streambank sites. Additionally, the adjusted R^2 values are much stronger, reinforcing the

assumption that the unstable banks were the outliers and that conditionally stable banks were equivalent to their stable counterparts.

The first derived equation, (e), is a positive relationship between bank height and the standard deviation of τ_c values on the bank. Similarly, equation (h) equates an increase in stream power to a taller streambank. These two interactions can be interpreted two different ways. One interpretation is that of an incising stream, which many of these have proven to be through comparison with the regional curve. This interpretation suggests that the banks are temporarily stable between events and the deviation in τ_c is partially responsible for erosion and bank failure, helping make streambanks taller. Likewise, the increase in stream power along a reach causes incision, therefore increasing erosion at the bed and subsequently increasing the bank height. The second interpretation of the bank height relationships is one that assumes the banks are stable in nature and natural deviations occur. As bank height increases, so does the span of soil types, moisture content, and other incontrollable factors all of which affect the critical shear stress of the in-situ soil matrix. Therefore, an increase in τ_c deviation about the mean occurs characteristically with subsequent bank height increases due to natural nonconformities. Likewise, taller banks are expected with larger bankfull stream power quantities due to a presumed increase in drainage area, and therefore larger base flow and higher average water surface. This heightened base flow water surface increases the confining pressure acting on the bank, allowing it to be taller opposed to banks in smaller watersheds with lower average flow depths. The fundamental answer to this complex relationship likely falls somewhere in between these two interpretations as it has been noted that the streams are incised, suggesting bank failure.

The critical shear stress was prominent in the multiple linear regression analysis of stable streambanks. This is because τ_c has been noted to control streambank erosion and resistance (Equation 1). The relationships (f) and (g) both suggest that the critical shear stress

increases as the stream power of the channel reach increases. Accounting for approximately 34% in the variance, this affiliation is more indicative of the conditions that streambanks become stable rather than a predictive tool for analyzing streambank properties. This suggests a geomorphologic relationship between the resistance at the bank and the energy in the stream similar to the basal endpoint control (Thorne, 1982). From this perspective, the energy in a system over time erodes the banks until they reach their critical strength. As bank failures occur due to imbalances in resistance and driving force, the amount of energy in the same flood event decreases due to changes in width in the channel. Eventually the system will reach a threshold where the force from the event will no longer cause erosion and the stream will stabilize. This is of course subject to debate, especially since this relationship only accounts for a third of the variance and considering the small sample size. However, this affiliation does have practical purposes in that as the known bankfull stream power in a system increases so must the resistant strength of the soil to compensate for the increased energy in order to maintain stability.

A clear relationship with the spatial structure of non-erodible components and the direct affiliation with bank stability was not obtained. Instead, the only major contribution to streambank interactions was found with the NN-slope in the regression equation (g) with the standard deviation of τ_c on streambanks accounting for 9% of variance. This affiliation with stability is dynamic and dependent on other contributing parameters (Figure 4 - 8).

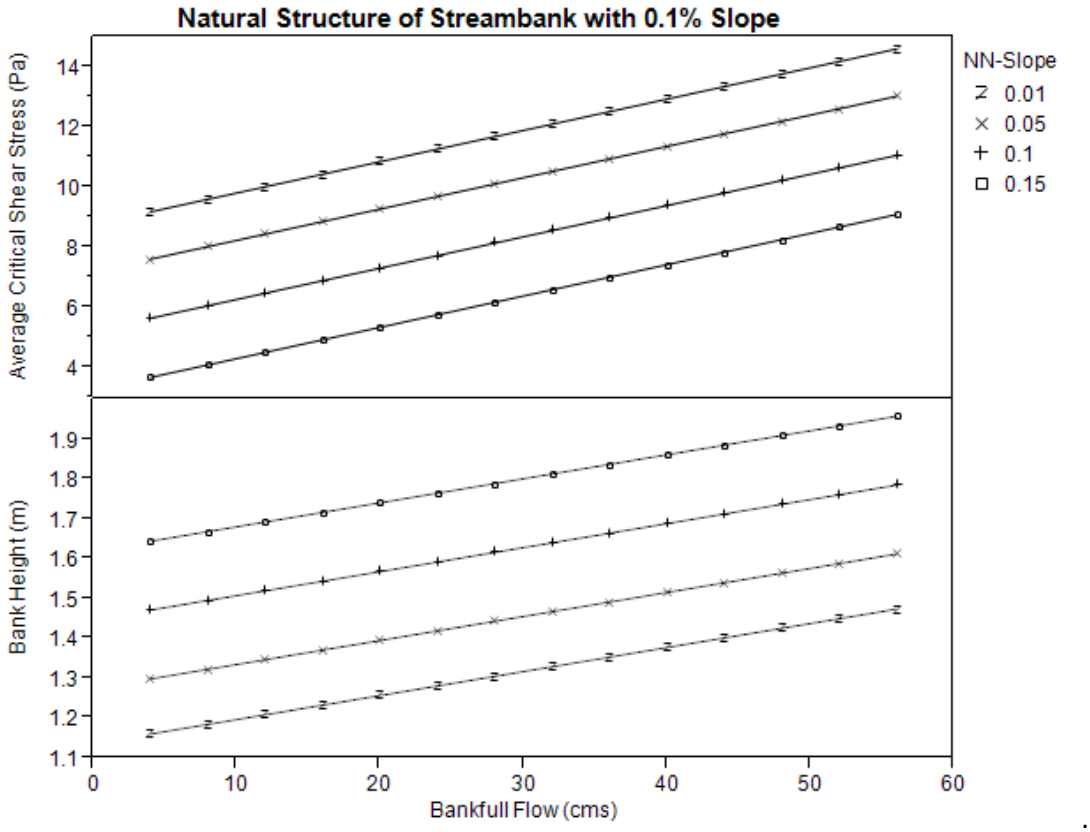

Figure 4 - 8: Graphical Representation of Stable Streambank Relationships

The interactions between these variables has been presented in Figure 4-8 with the purpose of visually describing the relationships derived in the multiple linear regression of stable streambanks. The parameter of streambank slope was set at a constant 0.1% gradient for the calculation purposes. It integrates streambank non-erodible clustering, soil resistance, bank geometry, and stream power principles to display the linear relationships between the variables. A figure similar to this could be developed for conceptual design purposes or general analyses of streambank stability in cohesive streambanks in the Eastern Tennessee Ridge and Valley Ecoregion.

Chapter V

Conclusion

The structure of natural streambanks is controlled by a complex set of parameters which cannot be predicted easily. This heterogeneous structure has been associated with the relative stability of the streambank in an attempt to conceptually understand what makes streambanks stable. To assess the relevancy of this research project the hypotheses presented in Chapter 4 must be readdressed.

The first hypothesis proposed that spatial structure of non-erodible components occurs naturally on streambanks and that there is a spatial dependence between them. This was tested using several spatial statistics and proven to be only slightly correct. According to the Clark and Evans (1954) aggregation index, nearest neighbor analysis, and join count methods it can be confidently stated that non-erodible structures cluster together. However, when determining the spatial dependence between these respective clusters using indicator variogram analysis, it was determined that only select banks develop a spatial dependence of these non-erodible aggregate regions. Furthermore, a statistical relationship in what causes this spatial dependence could not be adequately derived. It is believed that this spatial structure of non-erodible components is prevalent on streambanks; however, this investigation failed to realize this due to either a small sample size or the investigation being performed at an inappropriate scale.

The second proposed hypothesis suggested that streambanks naturally “armor” themselves to protect against the driving forces of fluvial erosion with a combination of non-erodible hard points and soil structure. Let us first consider the interaction between increased critical shear strength and increased clustering. It has been determined that a positive relationship exists between the two variables. A direct relationship relating the two parameters

and the energy in the stream was not obtained; however, the increase in stream power in a system was found to be associated with increase in the soils resistant strength. This signifies that the streambanks reach an equilibrium with the designated energy in the stream. It can be extrapolated that the clustering of non-erodible points helps increase this shear strength, however it cannot be stated in terms of statistical confidence.

The third hypothesis proposed that the stability of streambanks can be predicted, or conceptually understood, using all previously derived parameters. This was tested by removing the unstable banks from the analysis. It was determined that stable banks are controlled by a combination of the stream power, average critical shear of the stream bank and its distribution, bank height, and the non-erodible cluster density. These variables were integrated into a model to visually describe the interactions. Similar models could be applied to the design of natural channels or subsequent analysis of the stability of these channels.

This study provided unique information about the heterogeneous erodible and non-erodible stream bank structure and its interaction with bank stability and overall stream geomorphology. While the investigation derived several conclusions, it also stimulated many additional questions about the natural streambank environment. Additional research into the characteristics of natural streambanks and their interaction with non-erodible components is necessary to improve geomorphologic understanding and guidelines for stream restoration practices. This analysis considered spatial structure and periodicity of resistant components at the bank scale, finding that several banks possessed this quality. It is suggested that the periodicity may exist and be more prevalent at the reach scale, given by the spatial dependence of tree and boulder spacing. This may provide insight into geomorphologic evolution and potentially other results of stream degradation, such as suspended sediment. This study also failed to adequately represent moisture content changes in the soil structure. This ultimately affected the interactions with soil strength, stability and non-erodible structures. Future

investigations should better account for these variations and the overall influence on stability, soil structure, and spatial interactions. Another avenue of investigation would be to consider hydrologic watershed properties and their interaction with bank resistance. A simplified regional curve hydrologic relationship was used in this analysis to account for this; however, more detailed consideration of the hydrologic work done by catchment land use, soil characteristics, ground water, and regional precipitation would certainly provide a better understanding of streambank stability needs. Perhaps regional curves for streambank properties could be further developed to account for these parameters ultimately giving engineers stronger methods for natural channel design.

This research provided remarkable insight into the natural condition of streambank structure and its relationship with stability. The complexity of streambank non-erodible structure was prevalent in its relationship with the soil matrix; however, it was found not to contribute to the stability of the bank to the degree anticipated. In the end, it can be condensed to the primitive relationship of driving forces versus resisting forces. Thorne (1982) stated this concept best, “In nature no single process ever operates entirely alone to produce erosion.” Bank erosion is a mixture of all the controlling factors simultaneously working together and depending on local conditions, certain parameters become more significant than others. River bank stability is an intricate and important part of the hydrologic process and when, possible, should be maintained in order to promote the health of the river system.

List of References

Abernethy, B., Rutherfurd, I. D., 1998. Where along a river's length will vegetation most effectively stabilise stream banks?. Geomorphology, 23(1), 55-75.

Abernethy, B., Rutherfurd, I. D., 2001. The distribution and strength of riparian tree roots in relation to riverbank reinforcement. Hydrological processes, 15(1), 63-79.

Al-Madhhachi, A. T., Hanson, G. J., Fox, G. A., Tyagi, A. K., Bulut, R., 2013. Deriving parameters of a fundamental detachment model for cohesive soils from flume and Jet Erosion Tests. Transactions of the ASABE, 56(2), 489-504.

Al-Madhhachi, A. T., Hanson, G. J., Fox, G. A., Tyagi, A. K., Bulut, R., 2013. Measuring soil erodibility using laboratory “mini” JETs.”. T. ASABE, 56(3), 901-910.

Andrews, E. D., 1980. Effective and bankfull discharges of streams in the Yampa River basin, Colorado and Wyoming. J. Hydrology 46(3-4): 311-330.

ASCE Task Committee on Hydraulics, Bank Mechanics, and Modeling of River Width Adjust.1998. River Width Adjustment I: Processes and Mechanisms. Journal of Hydraulic Engineering 124(9): 881-902.

ASTM 1999b. Standard test method for liquid limit, plastic limit, and plasticity index of soils. No. D4318-84. American Society for Testing and Materials. West Conshohocken, PA. 4.08:526-538

Bagnold, R. A., 1966. An approach to the sediment transport problem from general physics. US Geol. Surv. Prof. Paper, 422, 231-291.

Blaisdell, F. W., Hebaus, G. G., Anderson, C. L., 1981. Ultimate dimensions of local scour. Journal of the Hydraulics Division, 107(3), 327-337.

Booth, D. B., 1990. Stream- channel incision following drainage basin urbanization. JAWRA Journal of the American Water Resources Association, 26(3), 407-417.

Beschta, R. L., Platts, W. S., 1986. Morphological features of small streams: significance and function. JAWRA Journal of the American Water Resources Association, 22(3), 369-379.

Brown, K., 2000. Urban stream restoration practices: an initial assessment. The Center for Watershed Protection. Ellicott City, Maryland, USA.

Bull, L. J., 1997. Magnitude and variation in the contribution of bank erosion to the suspended sediment load of the River Severn, UK. Earth Surface Processes and Landforms 22(12): 1109-1123.

Carline, R. F., Klosiewski, S. P., 1985. Responses of fish populations to mitigation structures in two small channelized streams in Ohio. North American Journal of Fisheries Management, 5(1), 1-11.

Casagrande, A., 1948. Plasticity chart for the classification of cohesive soils. Transactions of the American Society of Civil Engineers, 113, 901-930.

Clark, P. J., Evans, F. C., 1954. Distance to nearest neighbor as a measure of spatial relationships in populations. Ecology, 445-453.

Clark, L. A., Wynn, T. M., 2007. Methods for determining streambank critical shear stress and soil erodibility: Implications for erosion rate predictions. Transactions of the ASABE, 50(1), 95-106.

Cliff, A. D., Ord, J. K., 1981. Spatial processes: models & applications (Vol. 44). London: Pion.

Croft, H., Anderson, K., Brazier, R. E., Kuhn, N. J., 2013. Modeling fine-scale soil surface structure using geostatistics. Water Resources Research, 49(4), 1858-1870.

Davis, John C., 2002. Statistics and Data Analysis in Geology. New York: Wiley, Print.

Darby, S., Thorne, C., 1996. Stability analysis for steep, eroding, cohesive riverbanks. Journal of Hydraulic Engineering 122(8): 443-454.

Donnelly, K., 1978. Simulations to determine the variance and edge-effect of total nearest neighbor distance. Simulation methods in archaeology, 91-95.

Eaton, B. C., Giles, T. R., 2009. Assessing the effect of vegetation-related bank strength on channel morphology and stability in gravel-bed streams using numerical models. Earth Surface Processes and Landforms 34(5): 712-724.

El-Ramly, H., Morgenstern, N. R., Cruden, D. M., 2002. Probabilistic slope stability analysis for practice. Canadian Geotechnical Journal, 39(3), 665-683.

Epperson, B. K., Alvarez-Buylla, E. R., 1997. Limited seed dispersal and genetic structure in life stages of Cecropia obtusifolia. Evolution, 275-282.

Fischenich, C., 2001. Stability thresholds for stream restoration materials. EMRRP Technical Notes Collection (ERDC TN-EMRRP-SR-29), U.S. Army Engineer Research Development Center, Vicksburg, MS. (http://el.erdc.usace.army.mil)

Fortin, M. J., Dale, M. R., Hoef, J., 2006. Spatial analysis in ecology. Encyclopedia of environmetrics.

Fox, G. A., Wilson, G. V., Simon, A., Langendoen, E. J., Akay, O., Fuchs, J. W., 2007. Measuring streambank erosion due to ground water seepage: correlation to bank pore water pressure, precipitation and stream stage. Earth Surface Processes and Landforms, 32(10), 1558-1573.

Goudie, A., 2013. Encyclopedia of Geomorphology. Routledge.

Hanson, G., 1990. Surface erodibility of earthen channels at high stresses. Part II-developing an in situ testing device. Transactions of the ASAE 33(1): 132-137.

Hanson, G., 1990. Surface erodibility of earthen channels at high stresses. Part I-open channel testing. Transactions of the ASAE 33(1): 127-131.

Hanson, G., Cook, K., 1997. Development of excess shear stress parameters for circular jet testing. ASAE Paper 972227.

Hanson, G., Cook, K., 2004. Apparatus, test procedures, and analytical methods to measure soil erodibility in situ. Applied engineering in agriculture 20(4): 455-462.

Hanson, G., Simon, A., 2001. Erodibility of cohesive streambeds in the loess area of the midwestern USA. Hydrological Processes 15(1): 23-38.

Harrelson, C.C., Potyondy, J.P., Rawlins, C.L., (1994) Stream Channel Reference Sites: An Illustrated Guide to Field Technique. General Technical Report. USDA, Forest Service, Fort Collins, Colorado.RM-245: 61 pp.

Hey, R., 1998. Frequency and Duration of Bankfull Flow and Application for Natural Channel Design. Engineering Approaches to Ecosystem Restoration: pp. 989-994.

Hungerford, L. L., 1991. Use of spatial statistics to identify and test significance in geographic disease patterns. Preventive Veterinary Medicine, 11(3), 237-242.

Isaaks, E. H., Srivastava, R. M., 1989. An introduction to applied geostatistics, Oxford University press New York.

Järvelä, J., 2002. Flow resistance of flexible and stiff vegetation: a flume study with natural plants. Journal of Hydrology, 269(1), 44-54.

Julien, P. Y., 2010. Erosion and sedimentation, Cambridge University Press.

Kanji, M. A., 1974. The relationship between drained friction angles and Atterberg limits of natural soils. Geotechnique, 24(4).

Klein, R. D., 1979. Urbanization and stream quality impairment1. JAWRA Journal of the American Water Resources Association, 15(4), 948-963.

Lacasse, S., Nadim, F., 1997. Uncertainties in characterising soil properties. Publikasjon-Norges Geotekniske Institutt 201: 49-75.

Langendoen, E. J., Simon, A., 2008. Modeling the evolution of incised streams. II: Streambank erosion. Journal of hydraulic engineering, 134(7), 905-915.

Lawler, D. M., 1995. The impact of scale on the processes of channel-side sediment supply: a conceptual model. IAHS Publications-Series of Proceedings and Reports-Intern Assoc Hydrological Sciences, 226, 175-186.

Mcpherson, J. B., 2011. Bankfull Geomorphic Relationships and Reference Reach Assessment of the Ridge and Valley Physiographic Province of East Tennessee. Thesis. University of Tennessee, Knoxville. Print.

Midgley, T. L., Fox, G. A., Heeren, D. M., 2012. Evaluation of the bank stability and toe erosion model (BSTEM) for predicting lateral retreat on composite streambanks. Geomorphology, 145, 107-114.

Mohamoud, Y., Sigleo, A. C., Parmar, R. S., 2009. Modeling the Impacts of Hydromodification on Water Quantity and Quality. US Environmental Protection Agency, Office of Research and Development, National Exposure Research Laboratory, Ecosystems Research Division.

Neitsch, S. L., Arnold, J. G., Kiniry, J. R., Williams, J. R., King, K. W., 2005. Soil and water assessment tool theoretical documentation version 2005. Texas, USA.

Niezgoda, S. L., Johnson, P. A., 2005. Improving the urban stream restoration effort: identifying critical form and processes relationships. Environmental Management, 35(5), 579-592.

Osman, A., Thorne, C., 1988. Riverbank Stability Analysis. I: Theory. Journal of Hydraulic Engineering 114(2): 134-150.

Osterkamp, W. R., Heilman, P., Lane, L. J., 1998. Economic considerations of a continental sediment-monitoring program. International Journal of Sediment Research, 13(4), 12-24.

Papanicolaou, A. N., Elhakeem, M., Hilldale, R., 2007. Secondary current effects on cohesive river bank erosion. Water resources research, 43(12).

Parker, C., Simon, A., Thorne, C. R., 2008. The effects of variability in bank material properties on riverbank stability: Goodwin Creek, Mississippi. Geomorphology, 101(4), 533-543.

Pollen, N., 2007. Temporal and spatial variability in root reinforcement of streambanks: accounting for soil shear strength and moisture. Catena 69(3): 197-205.

Rosgen, D. L., 1994. A Classification of Natural Rivers. Catena, 22:169-199.

Rosgen, D. L., 2007. Rosgen geomorphic channel design. Stream Restoration Design National Engineering Handbook Part, 654, 11-1.

Rossi, R. E., Mulla, D. J., Journel, A. G., Franz, E. H., 1992. Geostatistical tools for modeling and interpreting ecological spatial dependence. Ecological monographs, 62(2), 277-314.

Sherer, B. M., Miner, J. R., Moore, J. A., Buckhouse, J. C., 1992. Indicator bacterial survival in stream sediments. Journal of Environmental Quality, 21(4), 591-595.

Shields Jr, F. D., Copeland, R. R., Klingeman, P. C., Doyle, M. W., Simon, A., 2003. Design for stream restoration. Journal of Hydraulic Engineering, 129(8), 575-584.

Shields Jr, F. D., Knight, S. S., Cooper, C. M., 1994. Effects of channel incision on base flow stream habitats and fishes. Environmental Management, 18(1), 43-57.

Simon, A., Collison, A. J., 2002. Quantifying the mechanical and hydrologic effects of riparian vegetation on streambank stability. Earth Surface Processes and Landforms 27(5): 527-546.

Simon, A., Curini, A., Darby, S. E., Langendoen, E. J., 2000. Bank and near-bank processes in an incised channel. Geomorphology, 35(3), 193-217.

Simon, A., Hupp, C. R., 1986a. Channel evolution in modified Tennessee channels, Proc. Federral Interagency Sedimenation Conference, 4th, vol.2, 71-82.

Simon, A., Pollen-Bankhead, N., Thomas, R. E., 2011. Development and application of a deterministic bank stability and toe erosion model for stream restoration. Geophysical Monograph Series, 194, 453-474.

Simon, A., Rinaldi, M. 2006. Disturbance, stream incision, and channel evolution: The roles of excess transport capacity and boundary materials in controlling channel response. Geomorphology. 79:361-383.

Smerdon, E. T., Beasley, R. P., 1961. Critical tractive forces in cohesive soils. Agricultural Engineering, 42(1), 26-29.

Stein, O. R., Nett, D. D., 1997. Impinging jet calibration of excess shear sediment detachment parameters. Transactions of the ASAE, 40(6), 1573-1580.

Thorne, C. R., 1982. Processes and mechanisms of river bank erosion. Gravel-bed rivers: 227-271.

Thorne, C. R., 1990. Effects of vegetation on riverbank erosion and stability. Vegetation and erosion, 125-144.

Thorne, C. R., Osman, A. M., 1988. Riverbank stability analysis. II: Applications. Journal of Hydraulic Engineering 114(2): 151-172.

Ullrich, C. R., Hagerty, D. J., Holmberg, R. W., 1986. Surficial failures of alluvial stream banks. Canadian Geotechnical Journal, 23(3), 304-316.

USEPA (United States Environmental Protection Agency), 2012. “Water Quality Standards History." Web. 02 Mar. 2014.

USEPA (United States Environmental Protection Agency), 2010. "Tennessee Water Quality Assessment Report." Web. 02 Apr. 2014.

Voight, B., 1973. Correlation between Atterberg plasticity limits and residual shear strength of manual soils. Geotechnique, 23(2).

Wesley, L. D., 2003. Residual strength of clays and correlations using Atterberg limits. Geotechnique, 53(7).

Wynn, T., Mostaghimi, S., 2006. The effects of vegetation and soil type on streambank erosion, Southwestern Virginia, USA. JAWRA Journal of the American Water Resources Association 42(1): 69-82.

Wynn, T. M., Mostaghimi, S., Burger, J. A., Harpold, A. A., Henderson, M. B., Henry, L. A., 2004. Variation in root density along stream banks. Journal of Environmental Quality, 33(6), 2030-2039.

Appendices

Appendix A: Calibration of the "Mini" Submerged Jet Test Device

The determination of the discharge coefficient,C, was completed in a laboratory investigation using a simplified modification of the energy equation. The ideal flow rate of the device was determined from the simplified nozzle equation,$Q = A\sqrt{2gh}$, while outflow from the device was measured. By examining the continuity of the flow over a range of pressure scales, C could effectively be quantified by determining the slope of measured discharge in relation to ideal discharge (Al-Madachi et al., 2013). A C = 0.9762 was achieved. This value is noticeably higher than the 0.7-0.8 range suggested by Al-Madachi et al (2013); however four unique methods were utilized in order to ensure the accuracy of the determination. The results and description of methodology are in Table A-1 and Figure A-1:

Table A - 1: Description of Methods Utilized in "Mini" Jet Test Calibration

Method	Description
1	Mini-jet tester connected to inline hose from pressurized water source. Outflow measured using floor scale and stopwatch.
2	Mini-jet tester connected to pump submerged in flume, to attempt to recreate field influent pressure. Outflow measured using floor scale and stopwatch.
3	Mini-jet tester connected to pump submerged in Tennessee River, in an attempt to simulate full field environment. Outflow measured using floor scale and stopwatch.
4	Mini- jet tester connected to pump in flume. Outflow measured with graduated cylinder to precisely measure outflow rates.

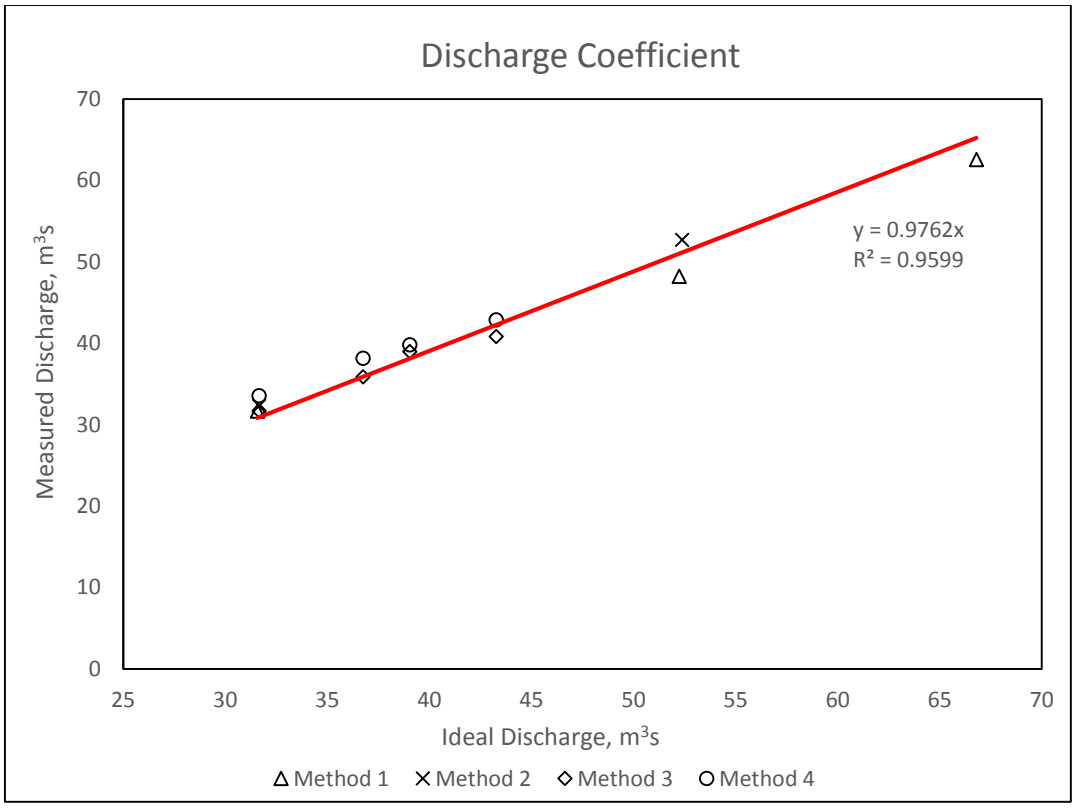

Figure A - 1: Discharge Coefficient Determination for the "Mini" Jet Test Device

Appendix B: Streambank Site Soil Data

Table B - 1: Streambank Atterberg Limits

Site	Top			Mid			Toe		
	LL	*PL*	*PI*	*LL*	*PL*	*PI*	*LL*	*PL*	*PI*
Beaver-1	32.2	15.6	16.6	38.7	17.5	21.2	43.7	21.5	22.2
Beaver-2	54.2	26.7	27.5	44.1	22.5	21.6	44.0	22.6	21.4
Beaver-3	49.9	27.0	22.8	42.4	21.8	20.5	40.7	21.3	19.4
Flat-1	38.1	21.4	16.7	44.1	24.6	19.5	42.0	25.1	16.9
Flat-2	33.8	20.2	13.6	31.3	17.0	14.3	51.4	28.3	23.1
Hinds-1	27.4	17.3	10.1	27.4	20.6	6.8	31.2	16.8	14.5
Hinds-2	28.8	18.9	9.9	27.4	16.2	11.1	28.0	19.4	8.5
Loves-1	32.1	20.7	11.4	38.6	21.3	17.3	27.0	17.3	9.7
Loves-2	34.4	21.5	12.9	33.3	20.3	13.0	26.9	17.2	9.8
Oostanaula-1	35.9	19.1	16.8	30.5	16.8	13.8	37.8	21.6	16.2
Oostanaula-2	40.2	21.2	19.0	34.8	18.3	16.5	35.9	16.9	19.1
Swan Pond-1	27.3	16.0	11.4	26.9	19.0	7.9	26.0	15.0	10.9
Swan Pond-2	31.5	16.0	15.6	39.9	20.8	19.1	46.8	22.7	24.0
Third-1	32.7	19.0	13.7	36.7	19.2	17.6	27.3	17.6	9.7
Third-2	32.2	18.0	14.3	33.8	17.3	16.5	29.7	20.6	9.0
Third-3	34.7	17.4	17.3	33.8	15.7	18.1	36.4	17.7	18.7
Walker Branch-1	27.9	17.8	10.1	25.0	14.2	10.8	30.5	17.8	12.8
Walker Branch-2	29.4	18.4	11.0	30.2	20.4	9.8	27.8	15.5	12.3

Table B - 2: Individual Jet Test Soil Erodibility Data for Streambank Sites

Site	Test #	Location	τ_c (pa)	k_d (cm^3/N-s)
Beaver1	1	Mid	23.432	0.348
Beaver1	2	Toe	8.519	0.493
Beaver1	3	Mid	7.160	0.472
Beaver1	4	Top	11.441	0.442
Beaver1	5	Top	5.287	1.048
Beaver1	6	Toe	17.361	0.275
Beaver1	7	Toe	12.742	0.310
Beaver1	8	Mid	7.704	2.488
Beaver1	9	Top	1.099	1.601
Beaver2	1	Mid	2.924	20.168
Beaver2	2	Mid	1.906	5.565
Beaver2	3	Toe	1.172	9.090
Beaver2	4	Toe	0.518	7.545
Beaver2	5	Top	0.545	3.345
Beaver2	6	Top	1.682	4.245
Beaver3	1	Top	3.249	1.612
Beaver3	2	Toe	18.221	0.320
Beaver3	3	Top	8.339	3.440
Beaver3	4	Mid	12.530	0.563
Beaver3	5	Mid	3.957	1.268
Beaver3	6	Toe	2.597	0.879
Beaver3	7	Top	1.887	0.861
Beaver3	8	Mid	1.961	1.142
Beaver3	9	Toe	30.248	0.316
Flat1	1	Mid	6.431	0.524
Flat1	2	Toe	1.120	1.018
Flat1	3	Top	0.433	3.179
Flat1	4	Top	0.413	10.511
Flat1	5	Toe	16.258	0.445
Flat1	6	Mid	6.736	0.789
Flat1	7	Toe	10.550	0.367
Flat1	8	Top	0.320	3.588
Flat1	9	Mid	14.579	0.279
Flat2	1	Toe	13.478	0.431
Flat2	2	Mid	28.141	0.327
Flat2	4	Toe	19.324	0.399
Flat2	5	Top	0.925	0.989
Flat2	6	Mid	48.544	0.095
Flat2	7	Toe	7.835	0.679
Flat2	8	Mid	44.602	0.174
Flat2	9	Top	0.446	4.514

Site	Test #	Location	τ_c (pa)	k_d (cm^3/N-s)
Hinds1	1	Mid	10.619	0.583
Hinds1	2	Toe	21.088	0.328
Hinds1	3	Toe	12.161	0.565
Hinds1	4	Mid	0.093	5.205
Hinds1	5	Top	4.832	1.762
Hinds1	6	Toe	22.846	0.393
Hinds1	7	Mid	1.399	3.349
Hinds1	8	Top	0.778	2.742
Hinds1	9	Top	0.309	8.425
Hinds2	1	Top	1.646	0.888
Hinds2	2	Toe	1.996	0.751
Hinds2	3	Mid	19.274	0.409
Hinds2	4	Mid	1.628	2.652
Hinds2	5	Mid	8.483	0.538
Hinds2	6	Top	15.290	0.316
Hinds2	7	Toe	0.727	2.862
Hinds2	8	Top	5.623	0.743
Hinds2	9	Toe	0.883	1.458
Loves1	1	Top	15.333	0.537
Loves1	2	Mid	5.049	1.354
Loves1	3	Toe	5.452	0.605
Loves1	4	Toe	0.410	1.388
Loves1	5	Mid	1.540	0.680
Loves1	6	Toe	8.692	0.548
Loves1	7	Mid	2.645	0.650
Loves1	8	Top	2.358	0.836
Loves1	9	Top	4.771	0.748
Loves2	1	Mid	21.792	0.270
Loves2	2	Top	17.879	0.488
Loves2	3	Top	11.717	0.527
Loves2	4	Toe	3.520	2.024
Loves2	5	Top	17.463	0.423
Loves2	6	Toe	13.272	0.491
Loves2	7	Mid	6.594	0.640
Loves2	8	Mid	18.037	0.533
Loves2	9	Toe	5.125	1.024
Oostanaula1	1	Top	9.641	1.577
Oostanaula1	2	Top	14.702	0.594
Oostanaula1	3	Mid	29.073	0.263
Oostanaula1	4	Mid	20.649	0.255
Oostanaula1	5	Toe	13.931	0.538
Oostanaula1	6	Top	3.717	0.768
Oostanaula1	7	Toe	14.444	0.339
Oostanaula1	8	Toe	27.388	0.218
Oostanaula1	9	Mid	1.009	0.901

Site	Test #	Location	τ_c (pa)	k_d (cm^3/N-s)
Oostanaula2	1	Toe	5.741	0.518
Oostanaula2	2	Top	0.143	1.968
Oostanaula2	3	Toe	1.976	0.710
Oostanaula2	4	Mid	3.604	0.747
Oostanaula2	5	Mid	12.612	0.674
Oostanaula2	6	Top	1.681	1.114
Oostanaula2	7	Mid	22.039	0.331
Oostanaula2	8	Top	0.285	2.326
Oostanaula2	9	Toe	29.269	0.189
SwanPond1	1	Mid	14.270	0.763
SwanPond1	2	Toe	22.082	0.312
SwanPond1	3	Toe	1.134	1.459
SwanPond1	4	Top	1.935	2.509
SwanPond1	5	Top	6.909	0.690
SwanPond1	6	Mid	16.884	0.560
SwanPond1	7	Top	5.103	0.698
SwanPond1	8	Mid	4.011	0.873
SwanPond1	9	Toe	21.216	0.322
SwanPond2	1	Top	11.329	1.577
SwanPond2	2	Toe	13.106	0.364
SwanPond2	3	Top	14.759	0.686
SwanPond2	4	Mid	5.818	1.047
SwanPond2	5	Toe	17.924	0.197
SwanPond2	6	Mid	10.003	1.457
SwanPond2	7	Mid	16.040	0.589
SwanPond2	8	Toe	18.176	1.009
SwanPond2	9	Top	18.544	0.342
Third1	1	Top	14.938	0.384
Third1	2	Toe	9.929	1.538
Third1	3	Top	11.537	0.626
Third1	4	Toe	6.097	1.601
Third1	5	Top	13.946	0.453
Third1	6	Toe	3.811	0.900
Third1	7	Top	15.963	0.311
Third1	8	Top	14.063	0.391
Third1	9	Top	14.479	0.636

Site	Test #	Location	τ_c (pa)	k_d (cm^3/N-s)
Third2	1	Toe	8.966	0.958
Third2	2	Top	19.756	0.221
Third2	3	Toe	6.524	1.010
Third2	4	Top	10.798	0.652
Third2	5	Top	19.286	0.229
Third2	6	Toe	15.459	1.284
Third2	7	Top	16.565	0.390
Third2	8	Toe	12.673	1.714
Third2	9	Top	8.350	0.412
Third3	1	Mid	19.282	0.480
Third3	2	Toe	2.156	1.083
Third3	3	Toe	4.935	2.000
Third3	4	Mid	25.482	0.990
Third3	5	Top	9.291	0.604
Third3	6	Toe	7.824	0.486
Third3	7	Top	20.706	1.828
Third3	8	Mid	4.507	1.409
Third3	9	Top	10.209	0.944
WalkerBranch1	1	Mid	6.854	2.077
WalkerBranch1	2	Toe	0.769	0.968
WalkerBranch1	3	Top	3.879	1.018
WalkerBranch1	4	Toe	1.266	2.053
WalkerBranch1	5	Toe	0.417	1.234
WalkerBranch1	6	Top	13.218	0.398
WalkerBranch1	7	Mid	3.924	1.187
WalkerBranch1	8	Top	0.438	2.254
WalkerBranch2	1	Mid	1.236	5.211
WalkerBranch2	2	Toe	5.121	1.342
WalkerBranch2	3	Toe	0.187	9.957
WalkerBranch2	4	Top	0.976	1.753
WalkerBranch2	5	Mid	1.129	1.841
WalkerBranch2	6	Top	1.892	4.672
WalkerBranch2	7	Mid	1.256	2.708
WalkerBranch2	8	Toe	0.417	2.642
WalkerBranch2	9	Top	2.235	2.177

Table B - 3: Streambank Soil Erodibility Values Averaged by Location

Bank	Location	$\tau_{c,avg}$ (pa)	$\tau_{c,stdev}$ (pa)	$k_{d,avg}$ (cm^3/N-s)	$k_{d,stdev}$ (cm^3/N-s)
Beaver1	Top	5.94	5.20	1.03	0.58
Beaver1	Mid	12.77	9.24	1.10	1.20
Beaver1	Toe	12.87	4.42	0.36	0.12
Beaver2	Top	1.11	0.80	3.80	0.64
Beaver2	Mid	2.41	0.72	12.87	10.33
Beaver2	Toe	0.84	0.46	8.32	1.09
Beaver3	Top	4.49	3.40	1.97	1.33
Beaver3	Mid	6.15	5.62	0.99	0.38
Beaver3	Toe	17.02	13.86	0.50	0.32
Flat1	Top	0.39	0.06	5.76	4.12
Flat1	Mid	9.25	4.62	0.53	0.26
Flat1	Toe	9.31	7.65	0.61	0.36
Flat2	Top	0.69	0.34	2.75	2.49
Flat2	Mid	40.43	10.82	0.20	0.12
Flat2	Toe	13.55	5.75	0.50	0.15
Hinds1	Top	1.97	2.49	4.31	3.60
Hinds1	Mid	4.04	5.74	3.05	2.33
Hinds1	Toe	18.70	5.73	0.43	0.12
Hinds2	Top	7.52	7.02	0.65	0.30
Hinds2	Mid	9.79	8.90	1.20	1.26
Hinds2	Toe	1.20	0.69	1.69	1.07
Loves1	Top	7.49	6.90	0.71	0.15
Loves1	Mid	3.08	1.79	0.89	0.40
Loves1	Toe	4.85	4.17	0.85	0.47
Loves2	Top	15.69	3.44	0.48	0.05
Loves2	Mid	15.47	7.92	0.48	0.19
Loves2	Toe	7.31	5.23	1.18	0.78
Oostanaula1	Top	9.35	0.52	0.98	0.52
Oostanaula1	Mid	16.91	14.40	0.47	0.37
Oostanaula1	Toe	18.59	7.63	0.37	0.16
Oostanaula2	Top	0.70	0.85	1.80	0.62
Oostanaula2	Mid	12.75	9.22	0.58	0.22
Oostanaula2	Toe	12.33	14.79	0.47	0.26
SwanPond1	Top	4.65	2.52	1.30	1.05
SwanPond1	Mid	11.72	6.80	0.73	0.16
SwanPond1	Toe	14.81	11.85	0.70	0.66
SwanPond2	Top	14.88	3.61	0.87	0.64
SwanPond2	Mid	10.62	5.14	1.03	0.43
SwanPond2	Toe	16.40	2.86	0.52	0.43
Third1	Top	14.15	1.48	0.47	0.14
Third1	Mid	-	-	-	-
Third1	Toe	6.61	3.09	1.35	0.39
Third2	Top	14.95	5.13	0.38	0.18
Third2	Mid	-	-	-	-
Third2	Toe	8.22	3.95	1.24	0.35
Third3	Top	13.40	6.34	1.13	0.63
Third3	Mid	16.42	10.78	0.96	0.47
Third3	Toe	4.97	2.83	1.19	0.76
WalkerBranch1	Top	5.85	6.61	1.22	0.94
WalkerBranch1	Mid	5.39	2.07	1.63	0.63
WalkerBranch1	Toe	0.82	0.43	1.42	0.57
WalkerBranch2	Top	2.66	2.18	2.59	1.82
WalkerBranch2	Mid	1.21	0.07	3.25	1.75
WalkerBranch2	Toe	1.91	2.78	4.65	4.64

Table B - 4: Average Soil Erodibility Data for all Streambank Sites

Bank	$\tau_{c,avg}$ *(Pa)*	$\tau_{c,stdev}$ *(Pa)*	*SW p-value**	$k_{d,avg}$ *(cm^3/N-s)*	$k_{d,stdev}$ *(cm^3/N-s)*	*SW p-value**
Beaver1	10.53	6.70	0.763	0.831	0.758	0.007
Beaver2	1.46	0.92	0.570	8.326	6.173	0.059
Beaver3	9.22	9.67	0.019	1.156	0.959	0.020
Flat1	6.32	6.30	0.093	2.300	3.320	0.001
Flat2	20.41	18.60	0.120	0.951	1.467	<0.0001
Hinds1	8.24	8.96	0.061	2.595	2.744	0.048
Hinds2	6.17	0.95	0.019	1.180	0.954	0.024
Loves1	5.14	4.56	0.094	0.816	0.328	0.011
Loves2	12.82	6.53	0.410	0.713	0.532	0.002
Oostanaula1	14.95	9.60	0.687	0.606	0.436	0.063
Oostanaula2	9.65	10.75	0.022	0.826	0.668	0.086
SwanPond1	10.39	8.28	0.165	0.909	0.689	0.015
SwanPond2	13.97	4.32	0.415	0.808	0.495	0.466
Third1	11.64	4.24	0.113	0.760	0.492	0.026
Third2	13.15	4.85	0.543	0.763	0.516	0.355
Third3	11.60	8.22	0.255	1.092	0.557	0.322
WalkerBranch1	3.85	4.41	0.032	1.399	0.657	0.346
WalkerBranch2	1.61	1.46	0.017	3.589	2.727	0.012

* SW p-value is from Shapiro-Wilk test for normality. H_o = samples come from normal distribution

Appendix C: Vegetation Selection for BSTEM

As stated in Section 2.2, it was not possible to measure all parameters for BSTEM in-situ. Therefore, an approximation of stream bank vegetation was constructed for each site based on site pictures, notes, and online descriptions. Due to the limitation in vegetation inputs within the BSTEM, vegetation was selected by applying a simplified process. Four categories of vegetation native to eastern TN were selected from the model parameters and each site was assigned its approximate vegetative cover based on the estimated cover amount and age of the species. A summary of the selection criteria in Table C-1 with color coordination assigned for species age/size. Itemized vegetation for each bank can be viewed in Table C-2:

Table C - 1: Vegetation Selection for BSTEM

Species	*Type*	*Small*	*Medium*	*Large*
Alder	Tree	5	15	25
Sweetgum, American	Tree	5	15	25
Switch Grass, Alamo	Grass	1	3	5
Sycamore, Eastern	Tree	5	15	25
Willow, Black	Tree	5	15	25

Table C - 2: Species Cover for Individual Sites for use in BSTEM

	Species Cover (%)					
Site	***Alder***	***Sweetgum***	***Switch Grass***	***Sycamore***	***Willow***	***Bare Soil***
Beaver-1	25	0	40	0	25	10
Beaver-2	25	0	20	25	0	30
Beaver-3	15	25	50	0	0	10
Flat-1	0	40	0	0	50	10
Flat-2	20	30	40	0	0	10
Hinds-1	40	30	20	0	0	10
Hinds-2	0	0	100	0	0	0
Loves-1	0	10	80	0	0	10
Loves-2	0	40	20	30	0	10
Oostanaula-1	0	0	40	0	50	10
Oostanaula-2	10	0	20	0	60	10
Swan Pond-1	30	0	10	20	30	10
Swan Pond-2	0	0	0	40	50	10
Third-1	10	0	0	0	80	10
Third-2	10	0	0	0	80	10
Third-3	40	0	0	0	50	10
Walker Branch-1	0	0	90	0	0	10
WalkerBranch-2	0	0	40	0	50	10

Appendix D: Modeling of the Indicator Semi-variogram

Adequately modeling the variogram with appropriate bounds is completed through a trial an error process. No explicit method exists to select the proper criteria for lag, lag distance, max lag distance; therefore, it must be completed in an arduous manner. The most important part of analyzing spatial data through variograms is first determining an appropriate lag size. Isaaks and Srivastava (1989) propose that for regularly sampled grids, such as the one in this experiment, the grid size match the lag size. This is a convenient measure, although it was desired to examine additional lag classes in order to best model the spatial data for interpretation of bank scale phenomena. Therefore, lag distances of 0.1, 0.2, and 0.5m were analyzed and modeled so that the lag with the most suitable structure could be used (Figure D-1).

The maximum lag distance is the extent of which the variogram models the spatial structure. This parameter is applied at the discretion of the user, and not strictly cited in literature. There is no mention of this parameter in Isaaks and Srivastava (1989) famous geostatistical text; however, Journey and Huijbregts (1978) suggest the ½ the maximum sampling distance be used since the quantity of pairs sampled beyond that point decrease, often rapidly, compromising the reliability of the relationship. Due to the concentrated density of the sampling effort, and the binary nature of the data, a significant amount of pairs exists at all lags. Therefore, the maximum variogram distance was extended to include 2/3 the total sampling distance so that a robust understanding of the changes in spatial structure could be achieved.

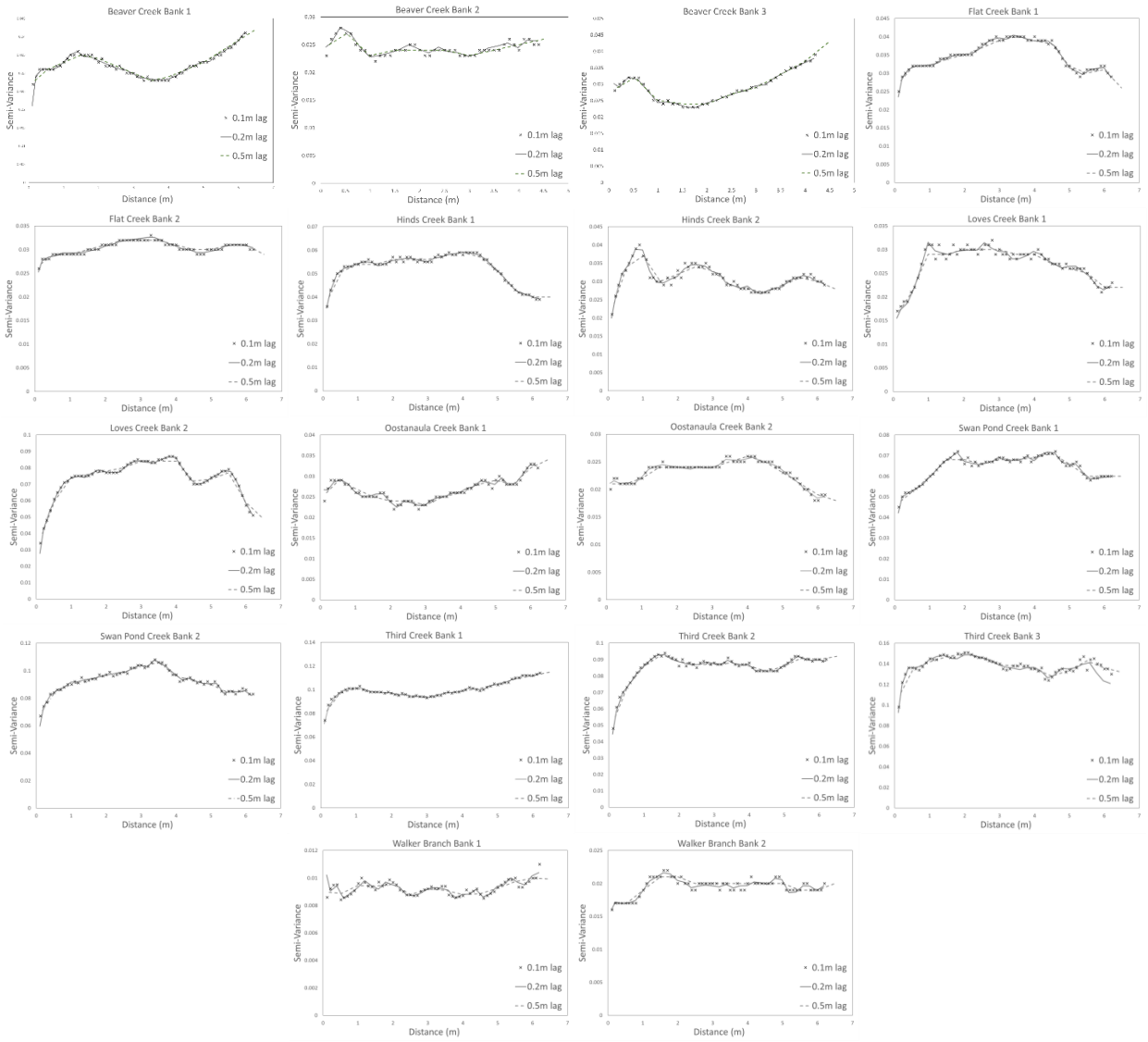

Figure D - 1 : Experimental Indicator Semi-Variograms at Unique Lag Classes

The 0.1m lag is quite noisy, representing every change in hard point variance along the bank while the 0.5 m variogram very crudely fits the overall structure of the variogram but does not count for any spatial patterns. The objective of spatially modeling the bank structures was to determine which sort of relationships exist at the bank scale. For this reason, 0.2 m lag was chosen because it accounts for micro-scale variability however eliminates the majority of noise so that more comprehensive trend analysis can be completed. In order to determine which lag

distance to use, one must first consider the resolution of which measurements occur, the scale of the plot and what the goal of the analysis is.

Three theoretical variogram models were fit to the dataset in an effort to formally parameterize the experimental variograms. They were Exponential, Gaussian, and Spherical models. Although the many of the theoretical variograms converged with the respective variograms with significant R^2 values, they did not pass the visual test also associated with the relevancy of this analysis. Therefore, it was decided that theoretical modeling of the variograms was not an acceptable solution.

Appendix E: Site Descriptions

Beaver Creek Bank 1

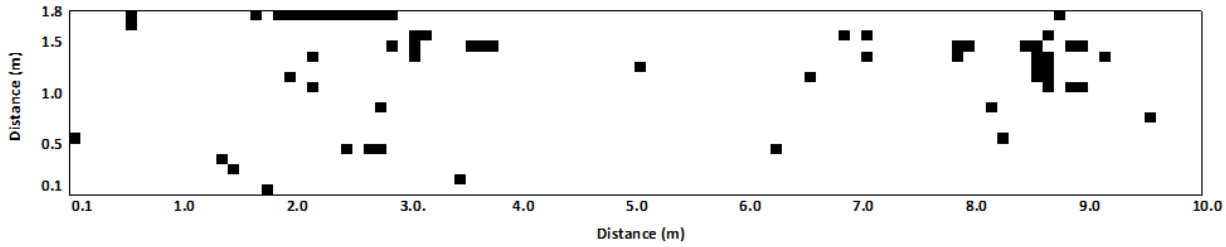

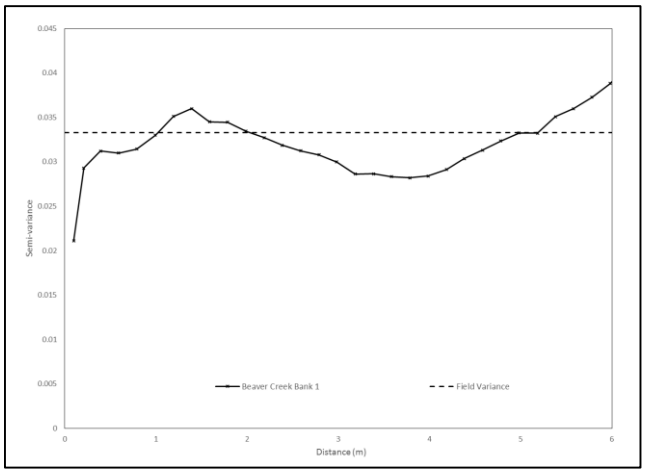

Variance	0.033
R	0.727
NN-Slope	0.099
% BB	0.61%
%WB	5.32%
Range	1.02
$\tau_{c,avg}$ **(Pa)**	10.5
$k_{d,avg}$ **(cm^3/N-s)**	0.8

Beaver Creek Bank 2

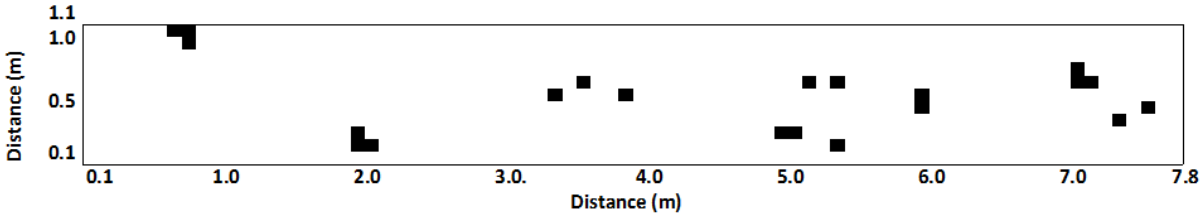

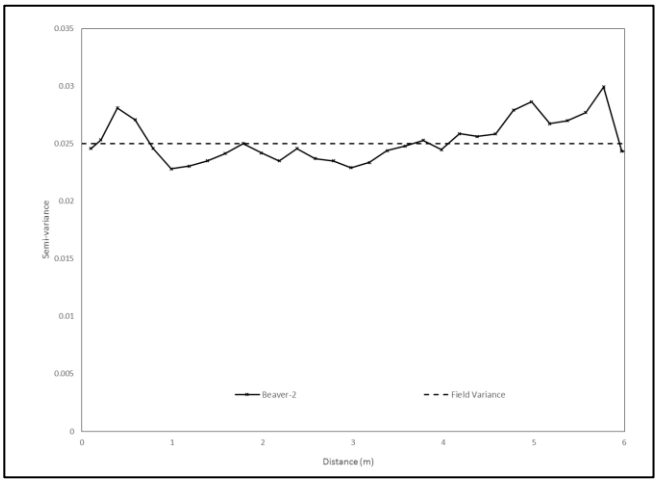

Variance	0.025
R	0.432
NN-Slope	0.241
% BB	0.35%
%WB	4.67%
Range	0.17
$\tau_{c,avg}$ **(Pa)**	1.5
$k_{d,avg}$ **(cm^3/N-s)**	8.3

Beaver Creek Bank 3

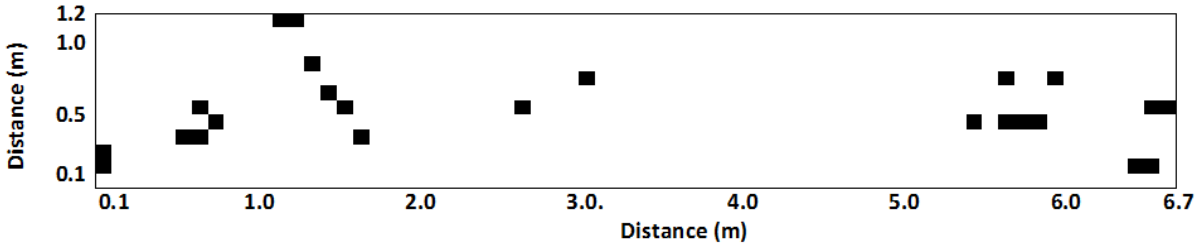

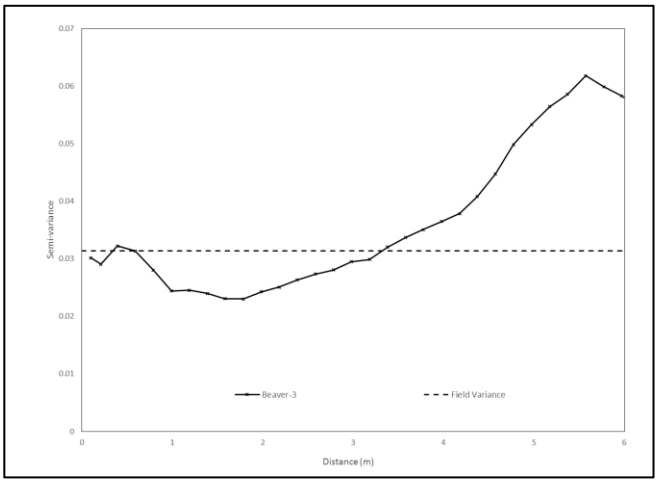

Variance	0.031
R	0.530
NN-Slope	0.124
% BB	0.40%
%WB	5.57%
Range	0.34
$\tau_{c,avg}$ (Pa)	9.2
$k_{d,avg}$ (cm^3/N-s)	1.2

Flat Creek Bank 1

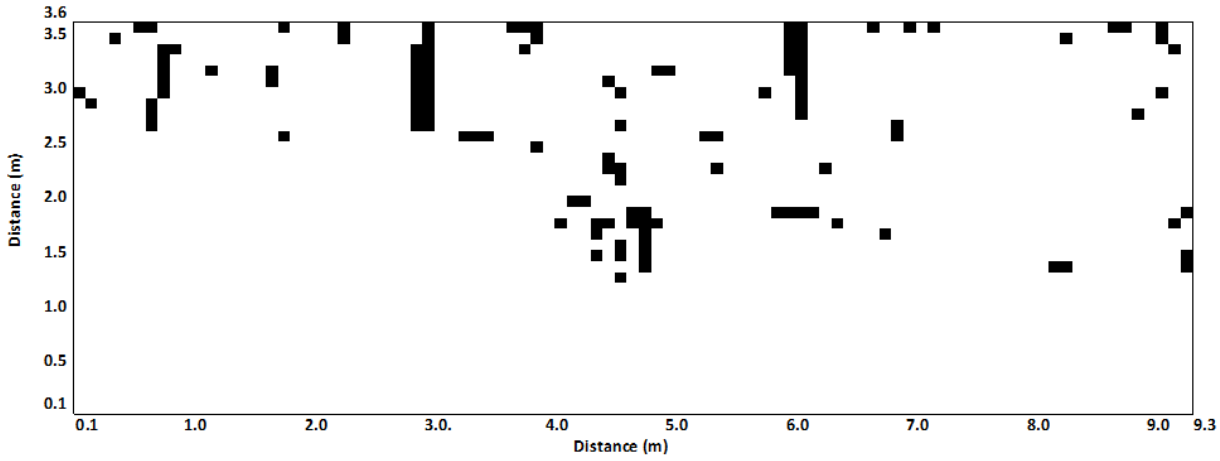

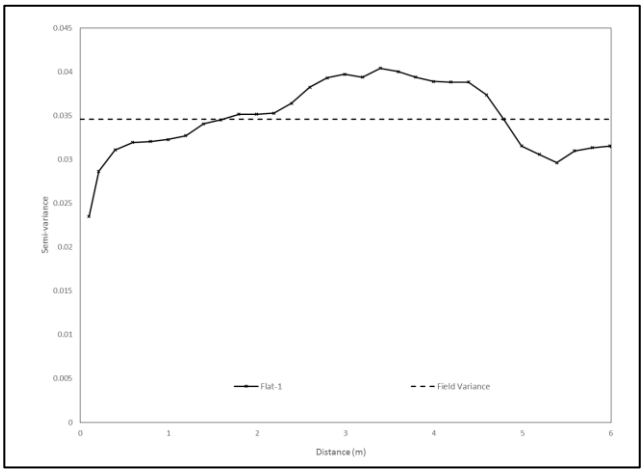

Variance	0.035
R	0.498
NN-Slope	0.077
% BB	0.94%
%WB	5.04%
Range	1.61
$\tau_{c,avg}$ **(Pa)**	6.3
$k_{d,avg}$ **(cm^3/N-s)**	2.3

Flat Creek Bank 2

N/A

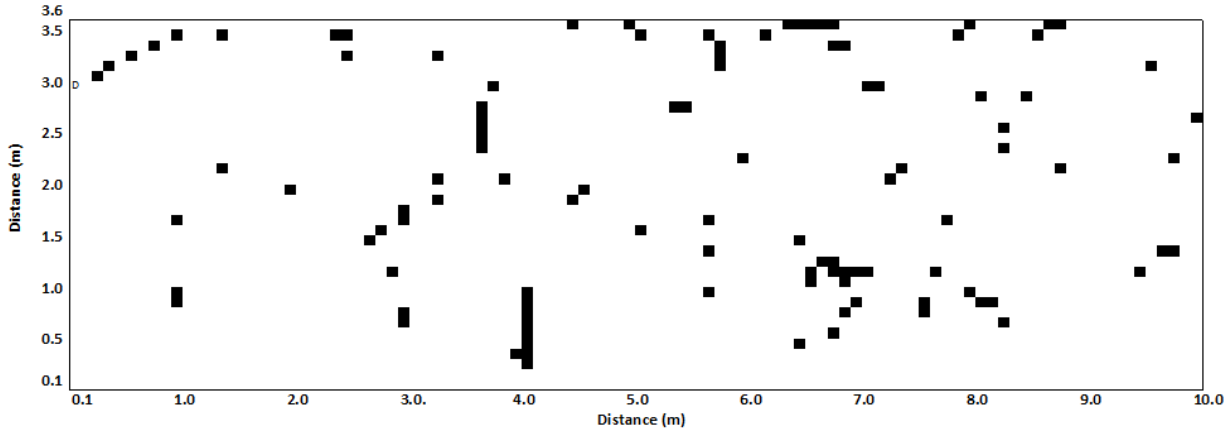

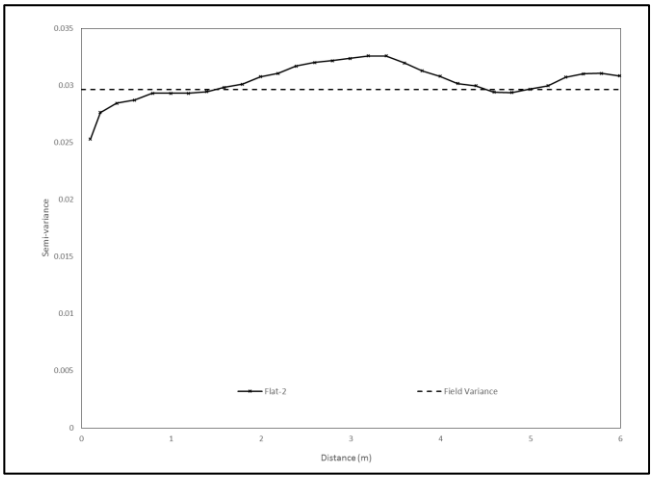

Variance	0.030
R	0.702
NN-Slope	0.125
% BB	0.39%
%WB	5.22%
Range	1.49
$\tau_{c,avg}$ **(Pa)**	20.4
$k_{d,avg}$ **(cm^3/N-s)**	1.0

Hinds Creek Bank 1

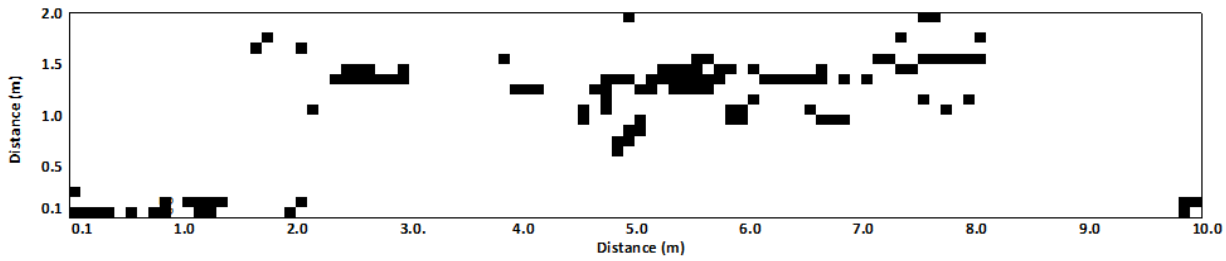

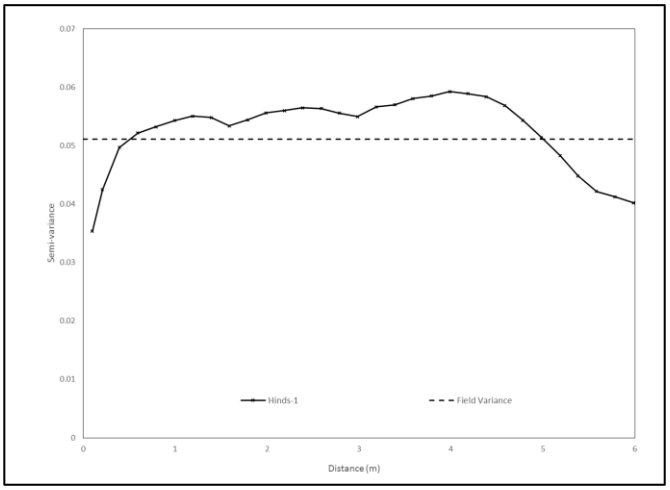

Variance	0.051
R	0.541
NN-Slope	0.068
% BB	1.74%
%WB	7.17%
Range	0.51
$\tau_{c,avg}$ (Pa)	8.2
$k_{d,avg}$ (cm^3/N-s)	2.6

Hinds Creek Bank 2

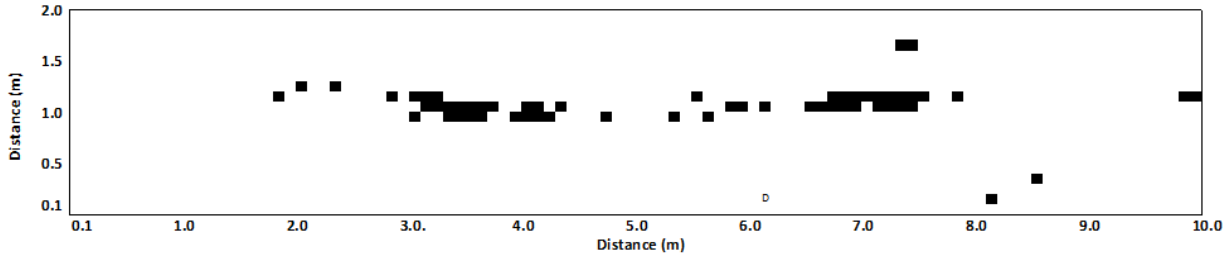

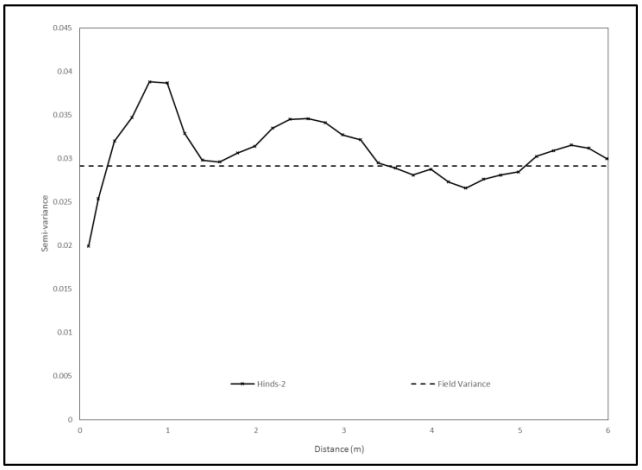

Variance	0.029
R	0.523
NN-Slope	0.065
% BB	1.05%
%WB	4.11%
Range	0.51
$\tau_{c,avg}$ (Pa)	6.2
$k_{d,avg}$ (cm^3/N-s)	1.2

Loves Creek Bank 1

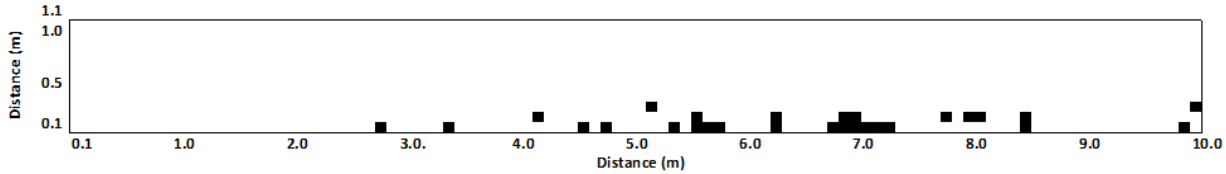

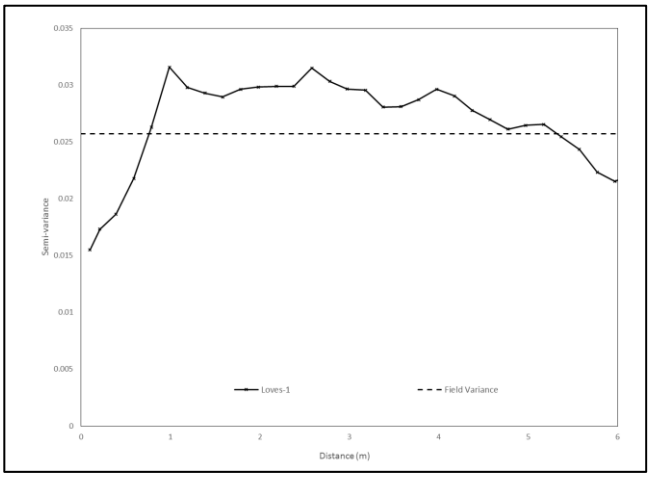

Variance	0.026
R	0.551
NN-Slope	0.131
% BB	0.47%
%WB	3.44%
Range	0.76
$\tau_{c,avg}$ **(Pa)**	5.1
$k_{d,avg}$ **(cm^3/N-s)**	0.8

Loves Creek Bank 2

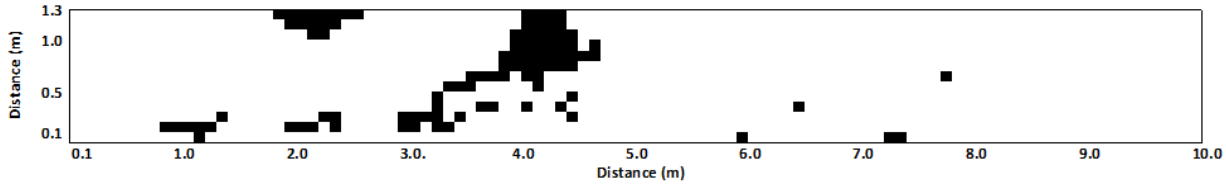

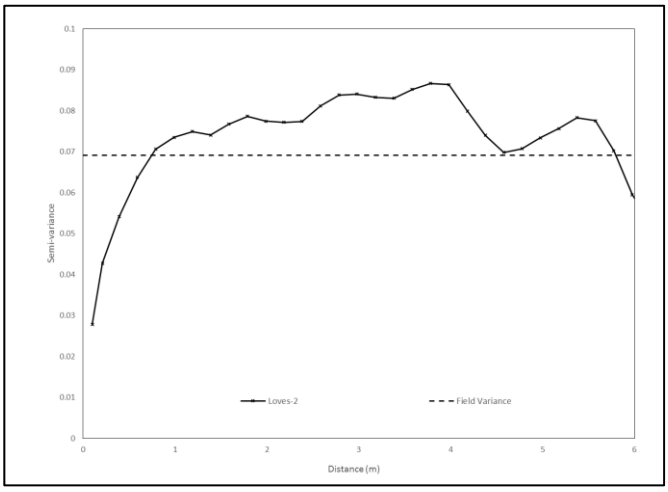

Variance	0.069
R	0.611
NN-Slope	0.050
% BB	4.05%
%WB	6.87%
Range	0.75
$\tau_{c,avg}$ (Pa)	12.8
$k_{d,avg}$ (cm^3/N-s)	0.7

Oostanaula Creek Bank 1

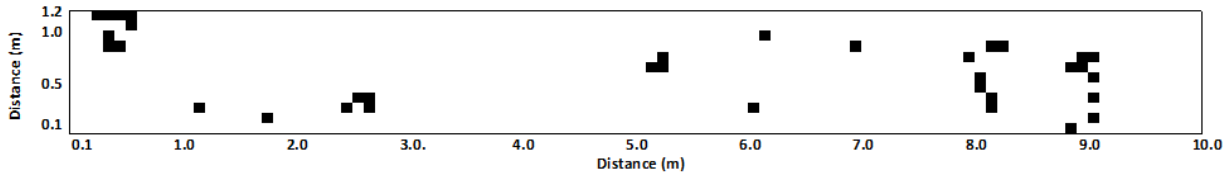

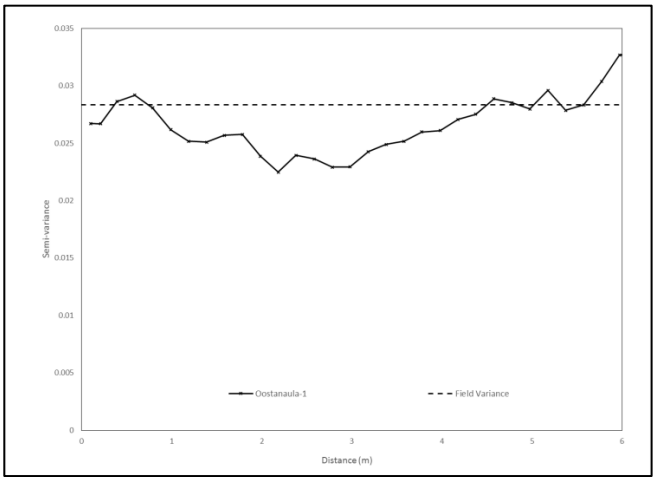

Variance	0.028
R	0.603
NN-Slope	0.129
% BB	0.56%
%WB	4.81%
Range	0.37
$\tau_{c,avg}$ (Pa)	15.0
$k_{d,avg}$ (cm^3/N-s)	0.6

Oostanaula Creek Bank 2

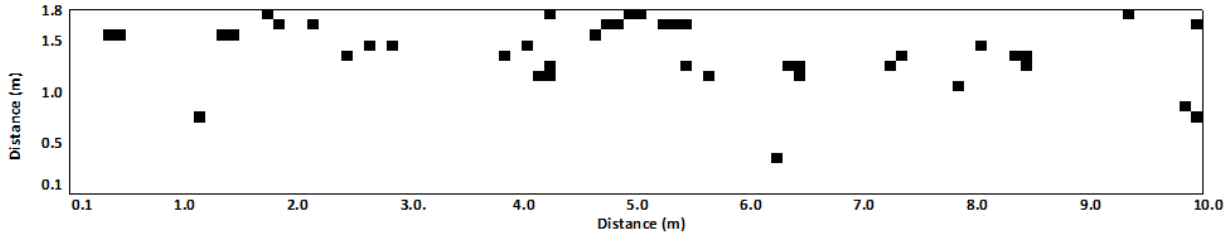

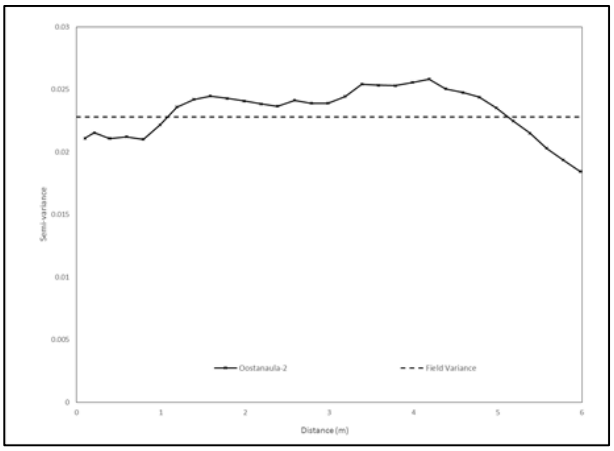

Variance	0.023
R	0.582
NN-Slope	0.149
% BB	0.29%
%WB	4.02%
Range	1.08
$\tau_{c,avg}$ (Pa)	9.7
$k_{d,avg}$ (cm^3/N-s)	0.8

Swan Pond Creek Bank 1

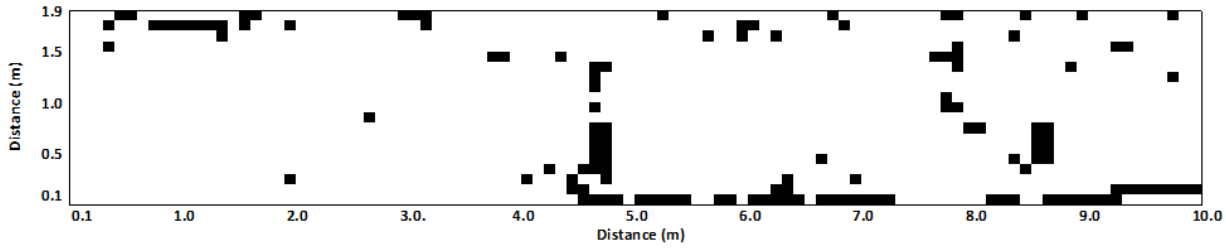

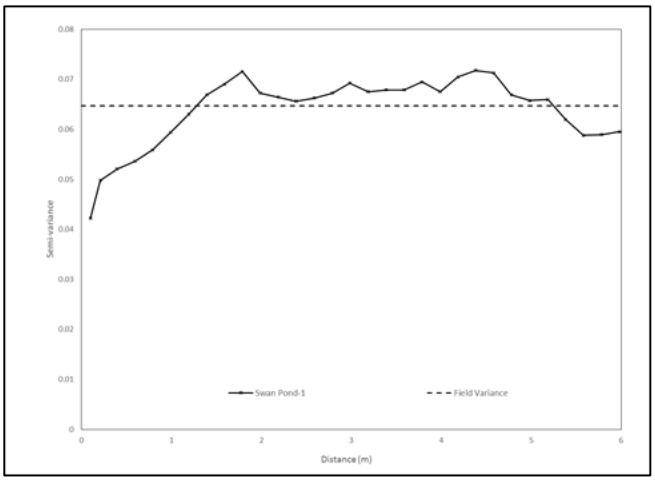

Variance	0.065
R	0.700
NN-Slope	0.070
% BB	1.79%
%WB	8.92%
Range	0.82
$\tau_{c,avg}$ **(Pa)**	10.4
$k_{d,avg}$ **(cm^3/N-s)**	0.9

Swan Pond Creek Bank 2

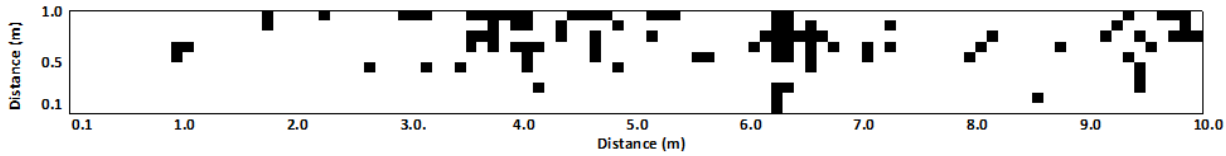

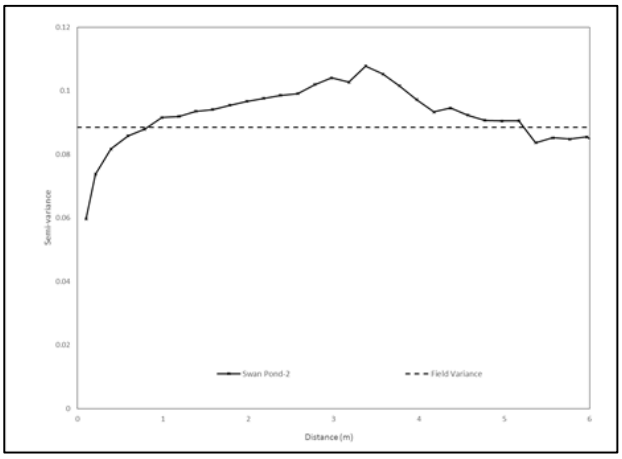

Variance	0.088
R	0.754
NN-Slope	0.062
% BB	2.89%
%WB	13.45%
Range	0.82
$\tau_{c,avg}$ (Pa)	14.0
$k_{d,avg}$ (cm^3/N-s)	0.8

Third Creek Bank 1

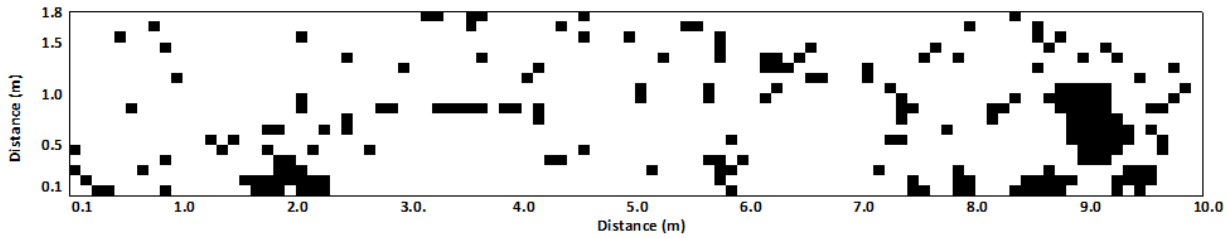

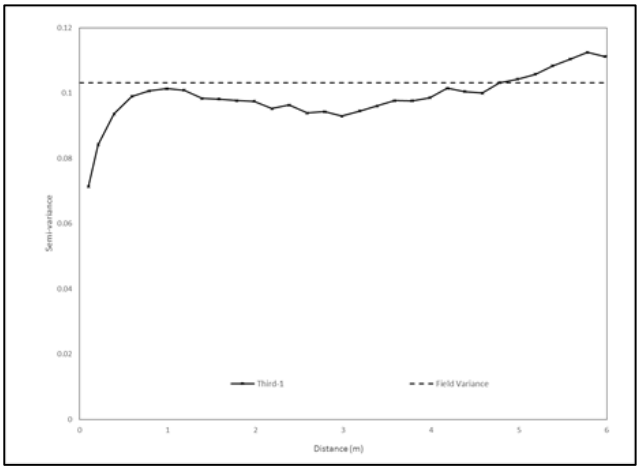

Variance	0.103
R	0.890
NN-Slope	0.049
% BB	4.22%
%WB	14.82%
Range	4.78
$\tau_{c,avg}$ (Pa)	11.6
$k_{d,avg}$ (cm^3/N-s)	0.8

Third Creek Bank 2

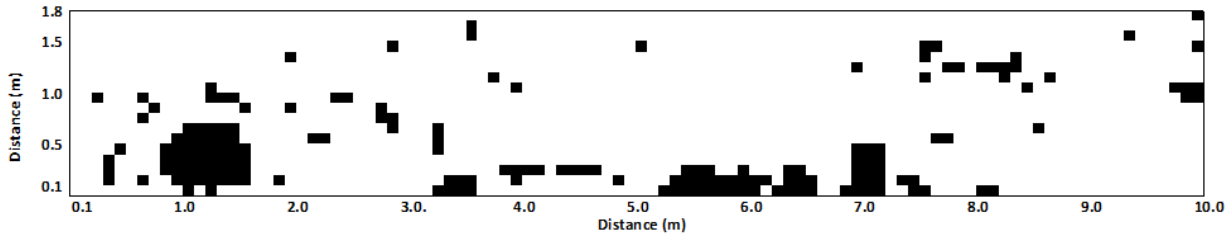

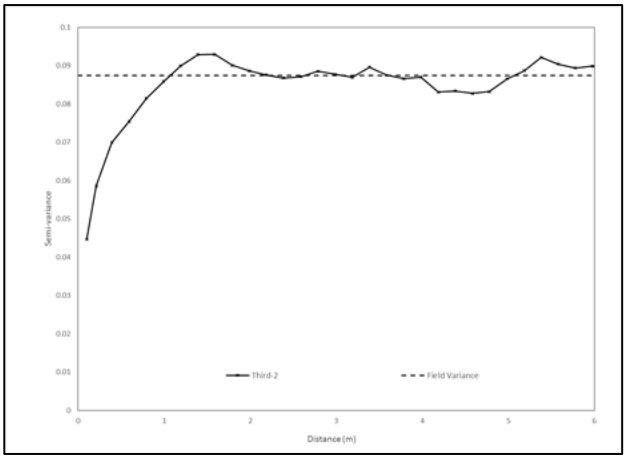

Variance	0.087
R	0.783
NN-Slope	0.040
% BB	4.69%
%WB	9.56%
Range	1.07
$\tau_{c,avg}$ (Pa)	13.2
$k_{d,avg}$ (cm^3/N-s)	0.8

Third Creek Bank 3

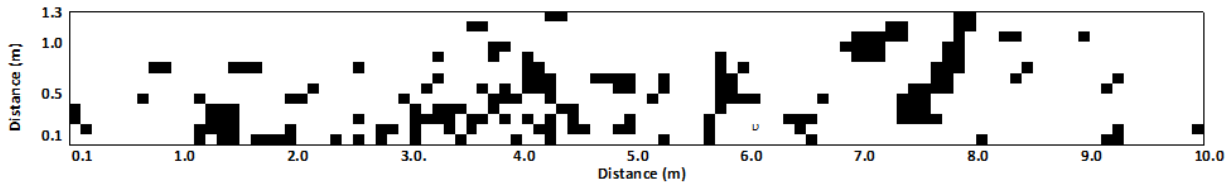

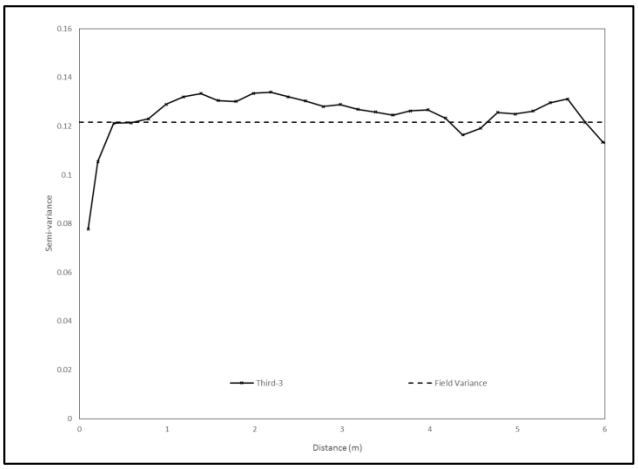

Variance	0.122
R	0.871
NN-Slope	0.043
% BB	5.70%
%WB	17.21%
Range	0.61
$\tau_{c,avg}$ (Pa)	11.6
$k_{d,avg}$ (cm^3/N-s)	1.1

Walker Branch Bank 1

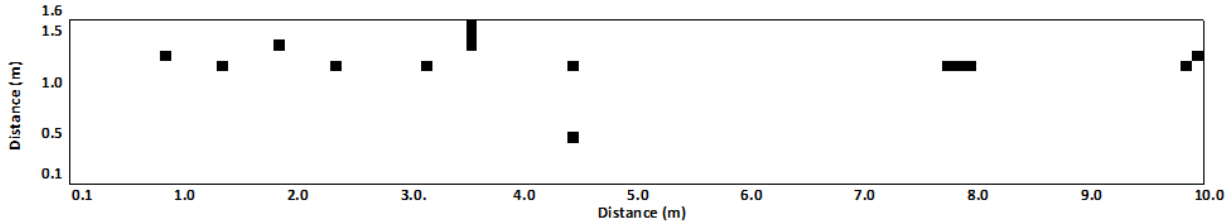

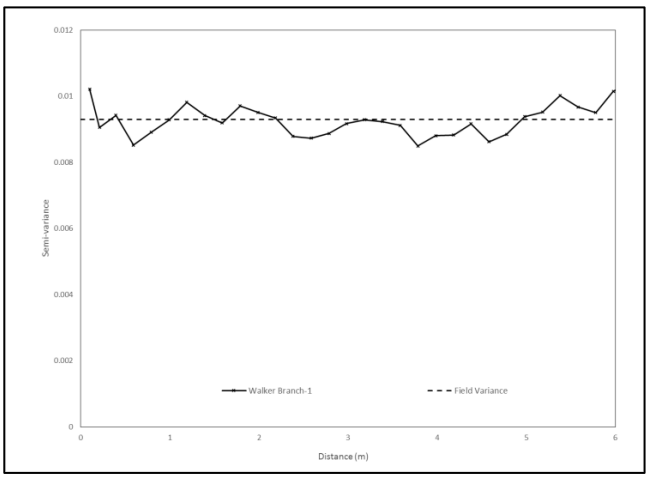

Variance	0.009
R	0.526
NN-Slope	0.511
% BB	0.08%
%WB	1.72%
Range	.
$\tau_{c,avg}$ (Pa)	3.8
$k_{d,avg}$ (cm^3/N-s)	1.4

Walker Branch Bank 2

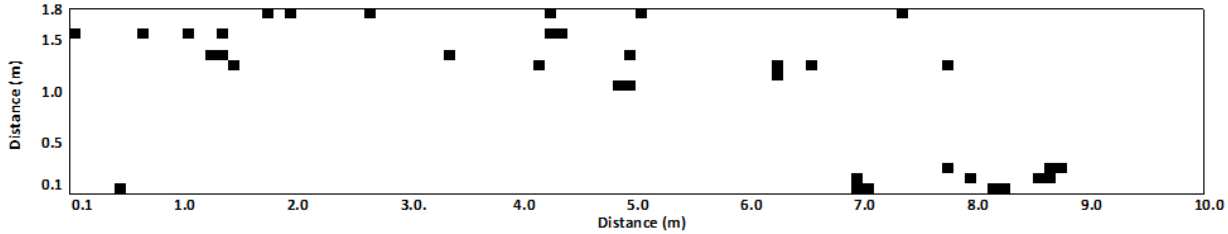

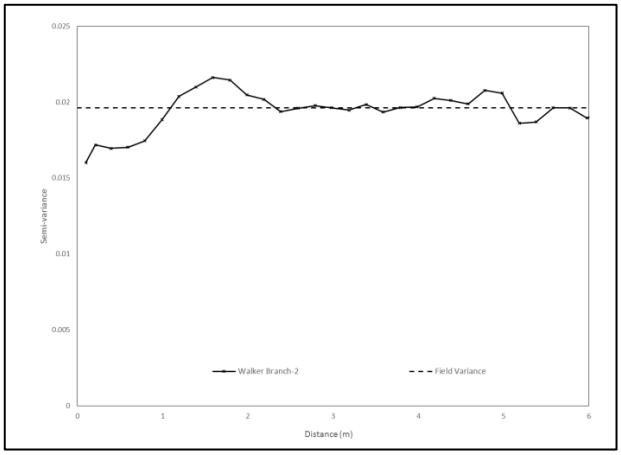

Variance	0.020
R	0.710
NN-Slope	0.153
% BB	0.20%
%WB	3.27%
Range	1.09
$\tau_{c,avg}$ (Pa)	1.6
$k_{d,avg}$ (cm^3/N-s)	3.6

Vita

Paul Vanterpool Simmons was born in Birmingham, Alabama on April 29, 1989. He received his elementary education in Vestavia Hills, Alabama and graduated from Vestavia Hills High School in 2007. In the fall of 2007, he began school at Auburn University studying Civil Engineering. While at Auburn, he was a co-op at the National Center for Asphalt Technology where he worked as a laboratory technician. He also worked under Dr. Jose Vasconcelos as an undergraduate research assistant participating a wide range of projects such as lab simulations of oil spill hydrodynamics in Mobile Bay, Alabama and hydrologic site analyses. Paul graduated from Auburn in May, 2012 with his Bachelors in Civil Engineering and enrolled as a master's student under the guidance of Dr. John Schwartz at the University of Tennessee in August, 2012. While at Tennessee, Paul took a leading role in the development of the 2013 UTK Stormwater Management Master Plan. Additionally, he participated in various field work activities for his thesis and an ongoing stream restoration project in Athens, TN.